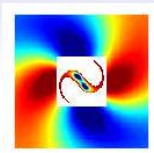

Turbulence and Noise Generation
Centre for Acoustics
LMFA, École Centrale de Lyon &
UMR CNRS 5509

On the use of high-order finite difference schemes in wall-bounded flow and acoustic problems.

Olivier Marsden , Ch. Bailly, Ch. Bogey
J. Berland, N. De Cacqueray, D. Desvigne

Centre Acoustique, Ecole Centrale de Lyon
LMFA, UMR CNRS 5509

http://acoustique.ec-lyon.fr

High-order Finite Differences : pros and cons

Pros

- naive versions are easy to program
- relatively easy to obtain arbitrarily high order derivative (and filtering) approximations
- amenable to whole-algorithm transfer function estimation

High-order Finite Differences : pros and cons

Pros

- naive versions are easy to program
- relatively easy to obtain arbitrarily high order derivative (and filtering) approximations
- amenable to whole-algorithm transfer function estimation

Cons

- at first sight, costly

  high order $\equiv$ large stencil size
- difficult to implement around (complex) geometries
  - non centred schemes are needed in the wall normal direction
  - painful to code (and therefore bug-prone)!

Plan

- Solving the Navier-Stokes equations with finite differences
  - Simulation approach
    - Navier-Stokes equations, curvilinear coordinates
  - High order Finite difference schemes
    - centred & non-centred
  - Dealing with multiple grids
- Illustrations
  - Cylindrical cavities
  - Infrasound propagation
  - Airfoil noise

Simulation approach

- Resolution of the full compressible Navier-Stokes equations in Cartesian & curvilinear coordinates
- Spatial discretization : high order explicit finite differences, typically fourth-order with 11 point stencils
- time integration : explicit 6-stage Runge-Kutta
- optimisation of finite differences, filtering and time stepping in the spatial and time frequency domains respectively
- LES methodology
  RF-LES : Relaxation Filtering, thanks to explicit high order filters.
  Effect of the smallest scales is assumed purely dissipative.

The Navier-Stokes equations in conservative form

$$\frac{\partial \mathbf{U}}{\partial t} + \frac{\partial E_i}{\partial x_i} - \frac{\partial V_i}{\partial x_i} = 0$$

$$\mathbf{U} = \begin{bmatrix} \rho \\ \rho u_1 \\ \rho u_2 \\ \rho u_3 \\ \rho e_t \end{bmatrix}$$

flow variables in conservative form

$$\mathbf{E}_i = \begin{bmatrix} \rho u_i \\ \rho u_1 u_i + p\delta_{1i} \\ \rho u_2 u_i + p\delta_{2i} \\ \rho u_3 u_i + p\delta_{3i} \\ u(\rho e_t + p) \end{bmatrix}$$

the Eulerian fluxes

$$\mathbf{V}_i = \begin{bmatrix} 0 \\ \tau_{i1} \\ \tau_{i2} \\ \tau_{i3} \\ u_j \tau_{ij} - q_i \end{bmatrix}$$

the visco-thermal fluxes

$$q_i = -\lambda \frac{\partial T}{\partial x_i}$$

$$\rho e_t = \frac{p}{\gamma - 1} \frac{1}{2} \rho u_i^2$$

$$\tau_{ij} = \mu \left(\frac{\partial u_i}{\partial x_j} + \frac{\partial u_j}{\partial x_i} - \frac{2}{3} \frac{\partial u_k}{\partial x_k} \right)$$

Curvilinear finite differences

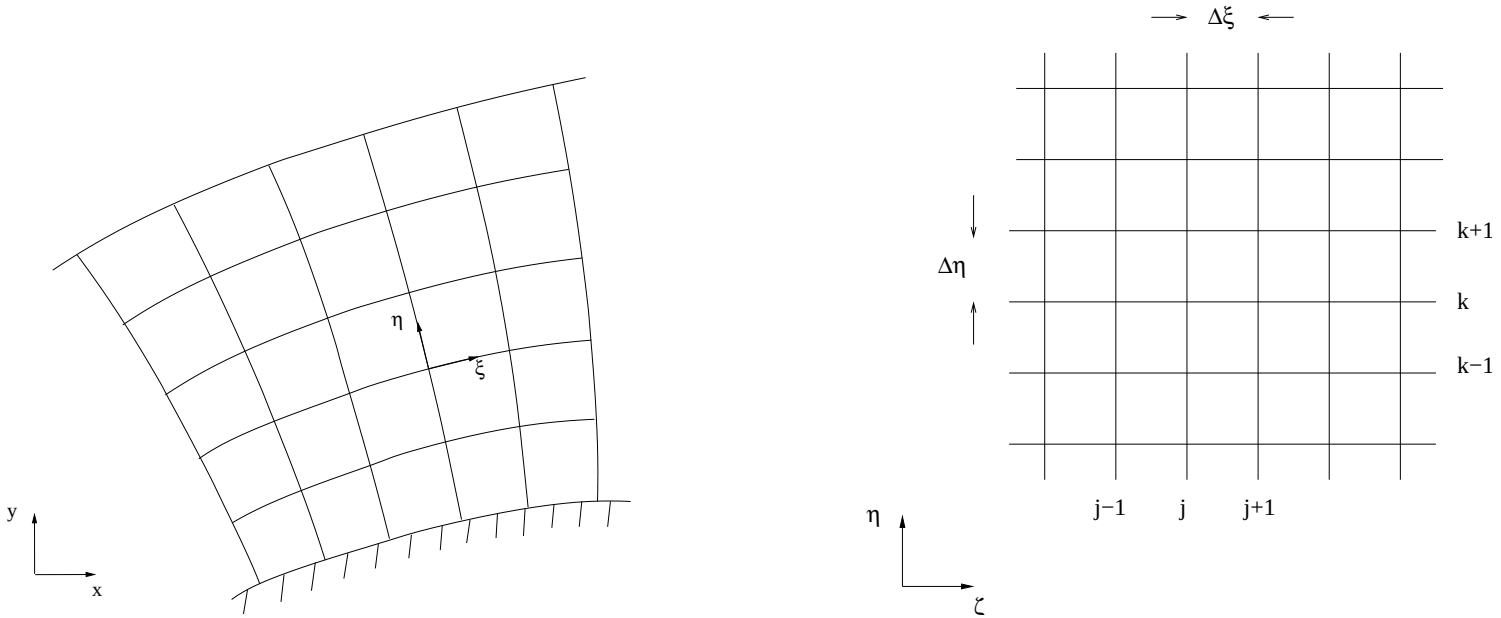

Physical (x, y) and transformed (ξ, η) domains

- Physical grid is body-fitted.
- Computational grid is Cartesian.

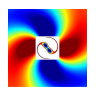

2D geometric transformation characteristics

Transformation characterized by its transformation matrix and Jacobian:

$$\mathbf{C} = \partial(\xi, \eta)/\partial(x, y), \; J = |C|$$

Equations to be solved:

$$\boxed{\frac{\partial \mathbf{U}^*}{\partial t} + \frac{\partial \mathbf{E}^*}{\partial \xi} + \frac{\partial \mathbf{F}^*}{\partial \eta} = 0}$$

$$\begin{aligned}
\mathbf{U}^* &= 1/J \; (\rho, \rho u, \rho v, \rho e_t)^T \\
\mathbf{E}^* &= 1/J \left(\frac{\partial \xi}{\partial x}(E_e - E_v) + \frac{\partial \xi}{\partial y}(F_e - F_v) \right)^T \\
\mathbf{F}^* &= 1/J \left(\frac{\partial \eta}{\partial x}(E_e - E_v) + \frac{\partial \eta}{\partial y}(F_e - F_v) \right)^T
\end{aligned}$$

The inverse transformation matrix $\mathbf{C}^{-1}$ is computed via finite difference schemes, and $\mathbf{C}$ is then reconstructed.

Finite differences on constant spacing grid

At each grid point, spatial derivatives such as $\frac{\partial E_m}{\partial x_n}$ are needed.

We approximate a derivative $\frac{\partial f}{\partial x}$ by finite differences :

$$\left.\frac{\partial f}{\partial x}\right|_i \simeq \frac{1}{\Delta x} \sum_{j=-m}^{n} a_j \cdot f(x_{i+j})$$

where the a_j are the scheme's coefficients.

The choice of the coefficients determines the scheme's properties.

Finite differences on constant spacing grid

A scheme's properties can be examined applying a Fourier transform $\hat{f}(k) = \frac{1}{2\pi}\int_{-\infty}^{\infty} f(x)e^{-ikx}dx$ to the previous approximation:

$$\begin{aligned} i\,k\,\hat{f} &\simeq \frac{1}{2\pi}\int_{-\infty}^{\infty}\frac{1}{\Delta x}\sum_{j=-m}^{n} a_j \cdot f(x+j\Delta x)e^{-ikx}dx \\ ik\hat{f} &\simeq \left(\frac{1}{\Delta x}\sum_{j=-m}^{n} a_j e^{i\,jk\Delta x}\right)\hat{f} \end{aligned}$$

The wavenumber computed by the scheme is then:

$$k^*(k) = -\frac{i}{\Delta x}\sum_{j=-m}^{n} a_j e^{ijk\Delta x}$$

For a periodic function of x, $f(x) = Ae^{ikx}$ the finite difference approximation of its derivative with the previously described scheme is

$$f'_{fd}(x) = ik^* f(x)$$

and $k - k^*$ can be called the scheme's error at this wavenumber.

Dissipation and dispersion of FD schemes

- $Re(k - k^*)$ relates to dispersion
- $Im(k - k^*)$ relates to amplification / dissipation

A necessary and sufficient condition for non-dissipative schemes is simply:

$$\sum_{j=-m}^{n} a_j e^{ijk\Delta x} \in i\mathcal{R} \Leftrightarrow a_j \text{ antisymetric}$$

Optimising FD schemes

Schemes can verify

- order conditions: the error function $k - k^*$ should behave like k^n , $n \geq 1$ for small k
- minimality conditions , *e.g.* $\int_{k_l}^{k_h} \left| ik - \sum_{j=-m}^{n} a_j e^{ijk\Delta x} \right|^2 dk$ should be minimal
- stability conditions

A set of properly chosen conditions then allows the scheme's coefficients to be computed with a Lagrange multiplier technique and matrix inversion.

Optimising FD schemes

A few examples of schemes built like this:

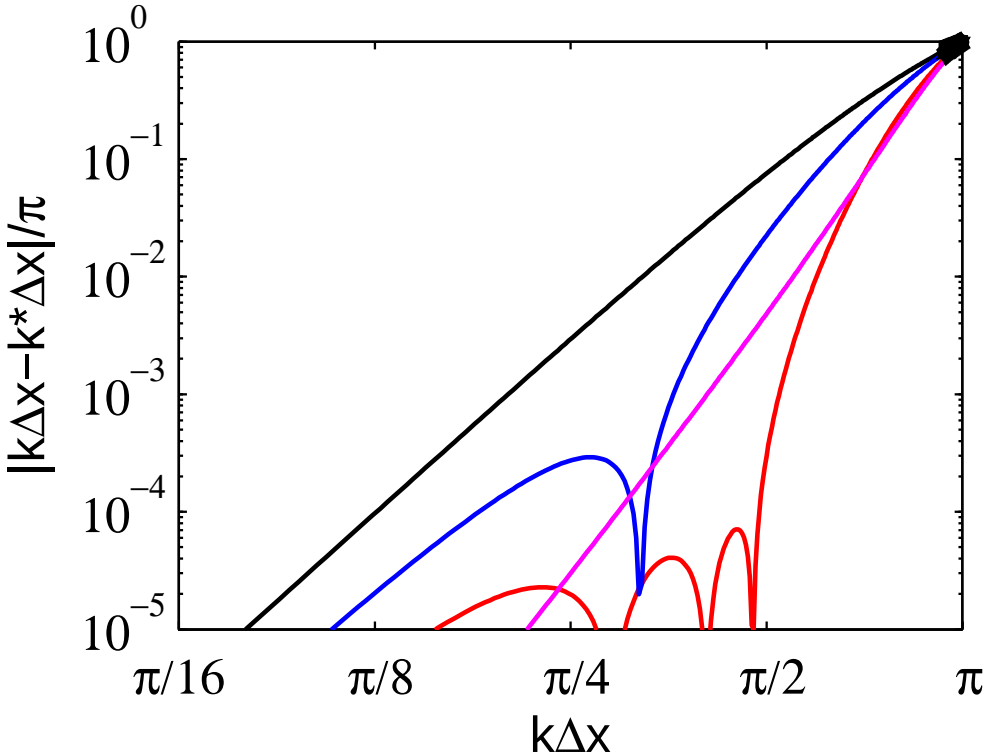

— standard 4th order , — 7 points DRP (Tam & Webb), — compact Lele,
— **11 points optimised**

Non-centred finite difference schemes

Close to boundaries, wide centred stencils can no longer be used.

- Centred reduced-width stencils have substantially degraded dispersion properties.
- With non-centred (wide) stencil, it is no longer possible to ensure $Im(k - k^*) = 0$ simply by choosing antisymetrical coefficients.

Non-centred finite difference schemes

Close to boundaries, wide centred stencils can no longer be used.

- Centred reduced-width stencils have substantially degraded dispersion properties.
- With non-centred (wide) stencil, it is no longer possible to ensure $Im(k - k^*) = 0$ simply by choosing antisymetrical coefficients.

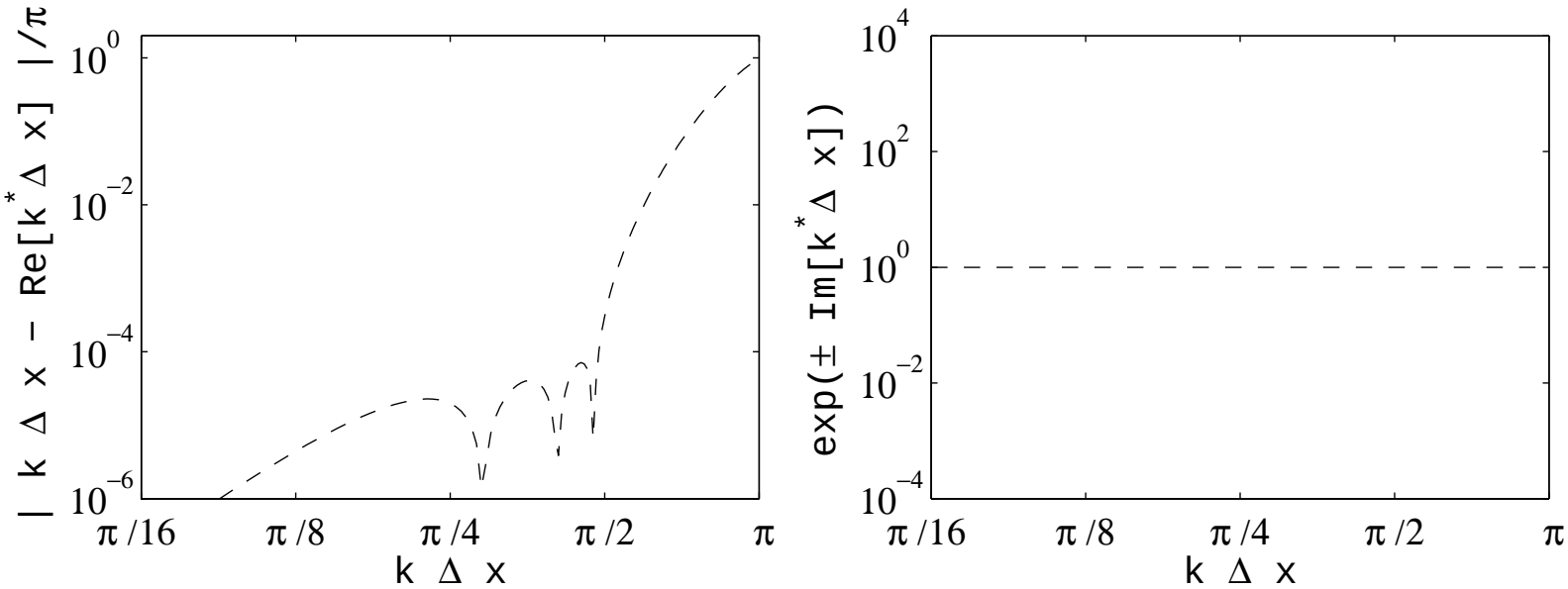

Dispersion and dissipation of finite difference schemes.

- - - reference centred 11-point.

Non-centred finite difference schemes

Close to boundaries, wide centred stencils can no longer be used.

- Centred reduced-width stencils have substantially degraded dispersion properties.
- With non-centred (wide) stencil, it is no longer possible to ensure $Im(k - k^*) = 0$ simply by choosing antisymetrical coefficients.

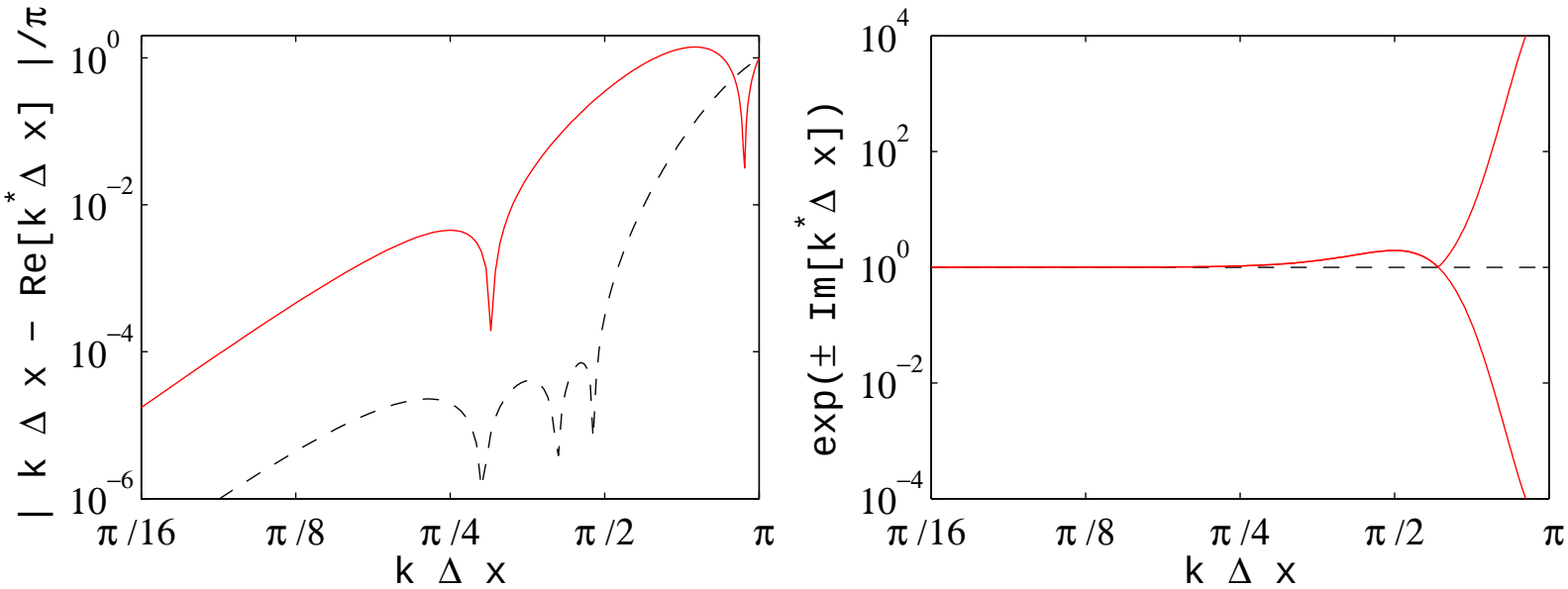

Dispersion and dissipation of finite difference schemes.

- - - reference centred 11-point, — 5-point fourth order at the wall.

Non-centred finite difference schemes

Close to boundaries, wide centred stencils can no longer be used.

- Centred reduced-width stencils have substantially degraded dispersion properties.
- With non-centred (wide) stencil, it is no longer possible to ensure $Im(k - k^*) = 0$ simply by choosing antisymetrical coefficients.

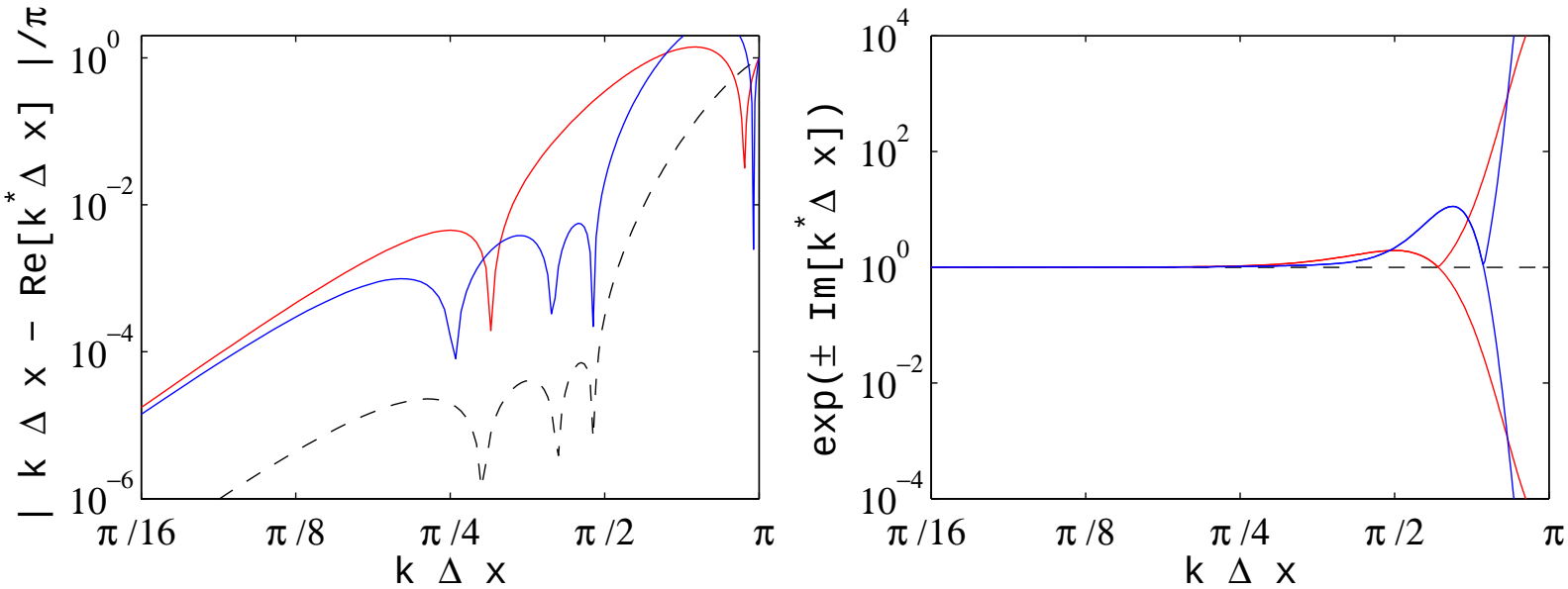

Dispersion and dissipation of finite difference schemes.

- - - reference centred 11-point, — 5-point fourth order,

— 7-point optimised at the wall.

Non-centred finite difference schemes

Close to boundaries, wide centred stencils can no longer be used.

- Centred reduced-width stencils have substantially degraded dispersion properties.
- With non-centred (wide) stencil, it is no longer possible to ensure $Im(k - k^*) = 0$ simply by choosing antisymetrical coefficients.

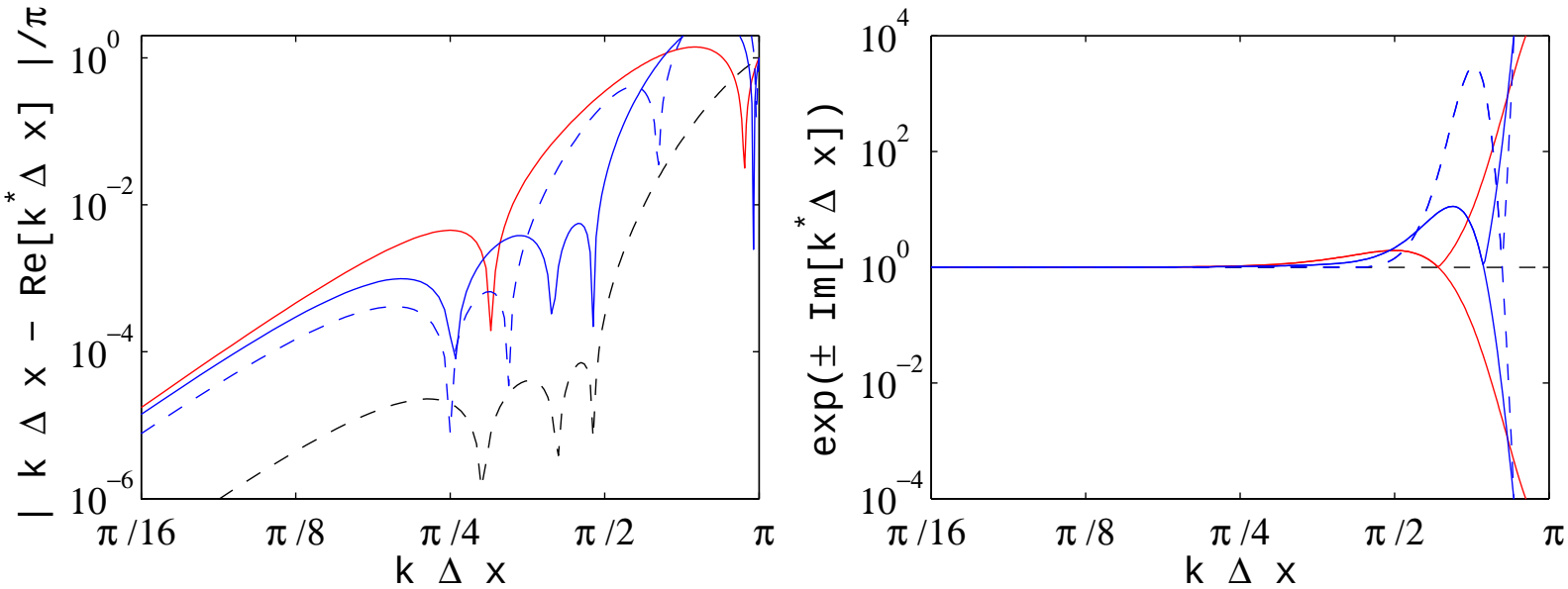

Dispersion and dissipation of finite difference schemes.
- - - reference centred 11-point, — 5-point fourth order,
— 7-point optimised, — 11-point optimised at the wall.

Non-centred finite difference schemes

Example of importance of non-centred schemes.

1D multiple reflection case.

Non-centred finite difference schemes

Example of importance of non-centred schemes.

1D multiple reflection case.

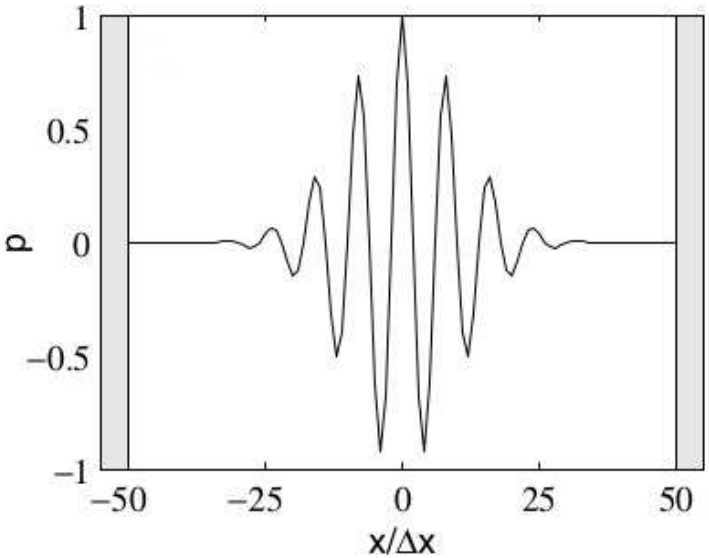

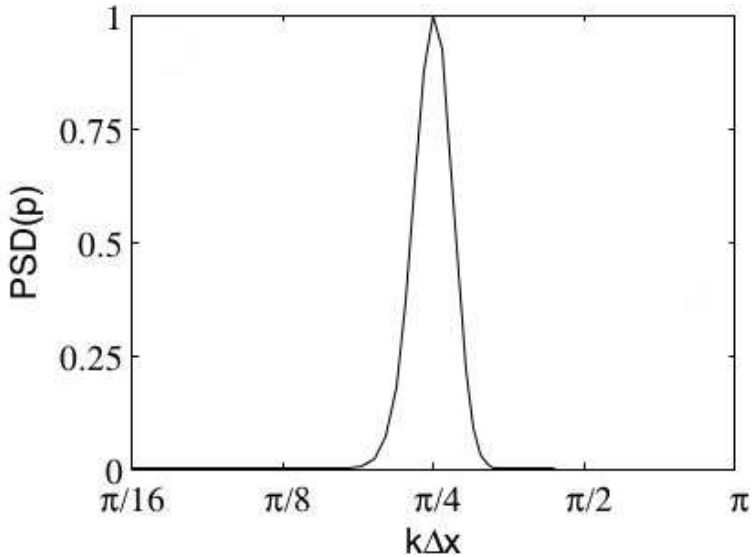

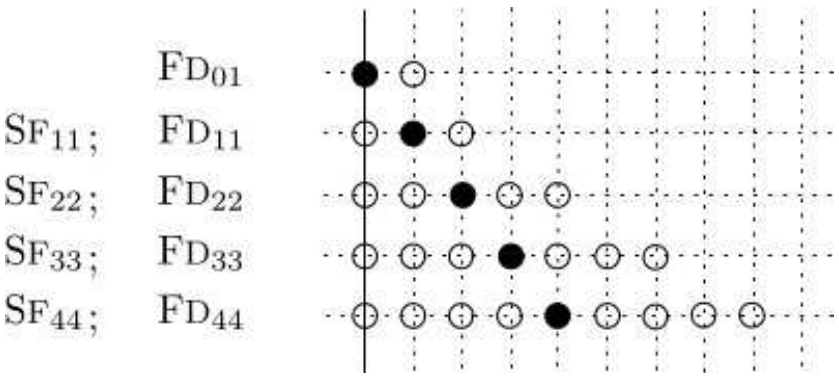

Wave packet reflects twice before reforming its original shape.

Berland et al., JCP 224 (2007)

Non-

Example of importance

Centred schemes and filters up to the wall.

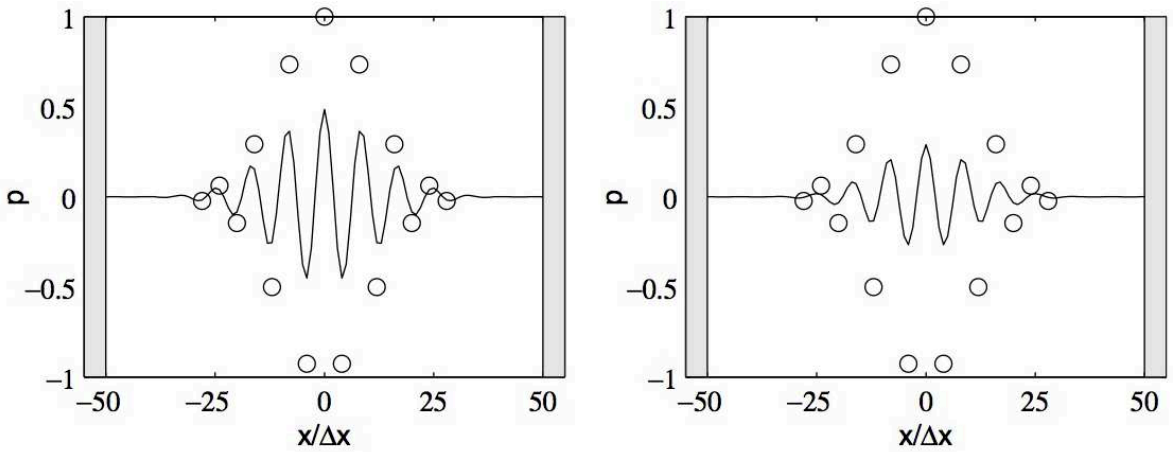

Non-cen

Example of importance of r

Centred schemes and filters up to the wall.

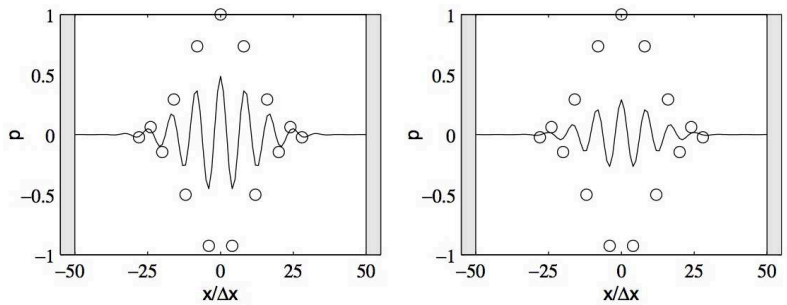

Wall point and next point with optimised schemes & filters.

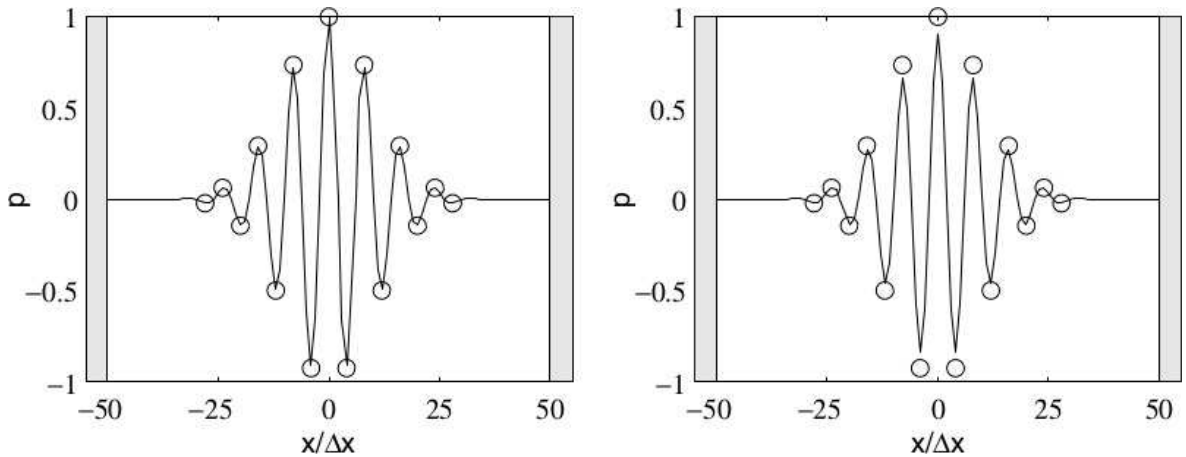

Non-cen

Example of importance of r

Centred schemes and filters up to the wall.

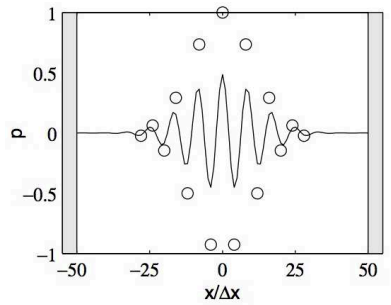

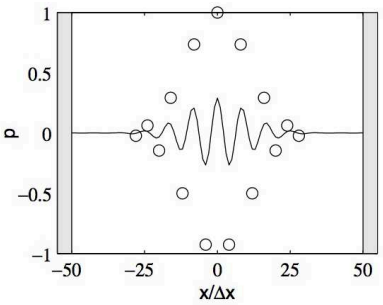

Wall point and next point with optimised schemes & filters.

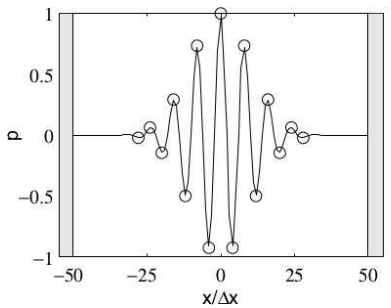

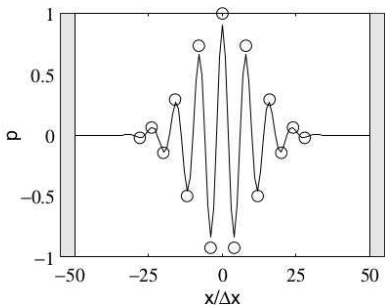

All non-centred optimised schemes & filters.

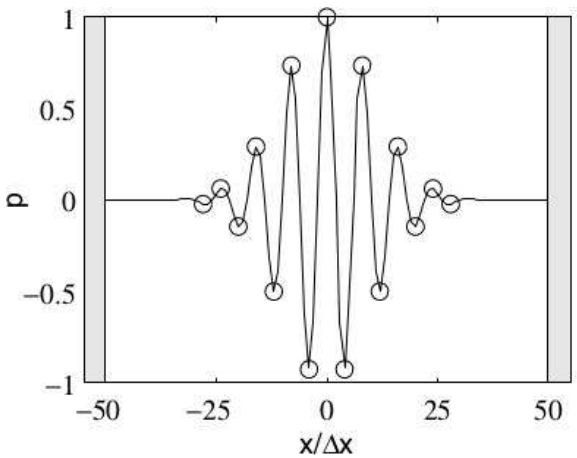

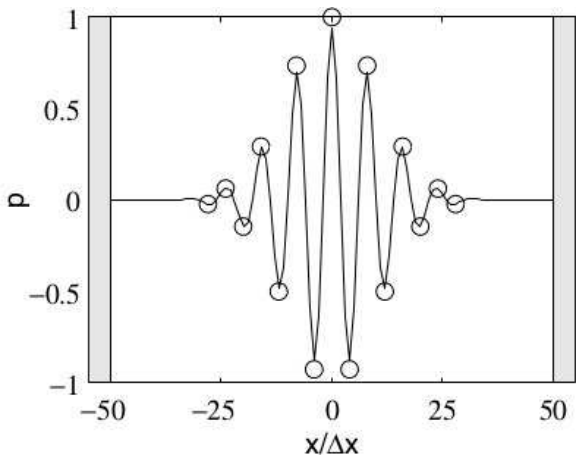

Non-centred finite difference schemes

Example of importance of non-centred schemes.

2D scattering problem, from the Second Computational Aeroacoustics Workshop.

Non-centred finite difference schemes

Example of importance of non-centred schemes.

2D scattering problem, from the Second Computational Aeroacoustics Workshop.

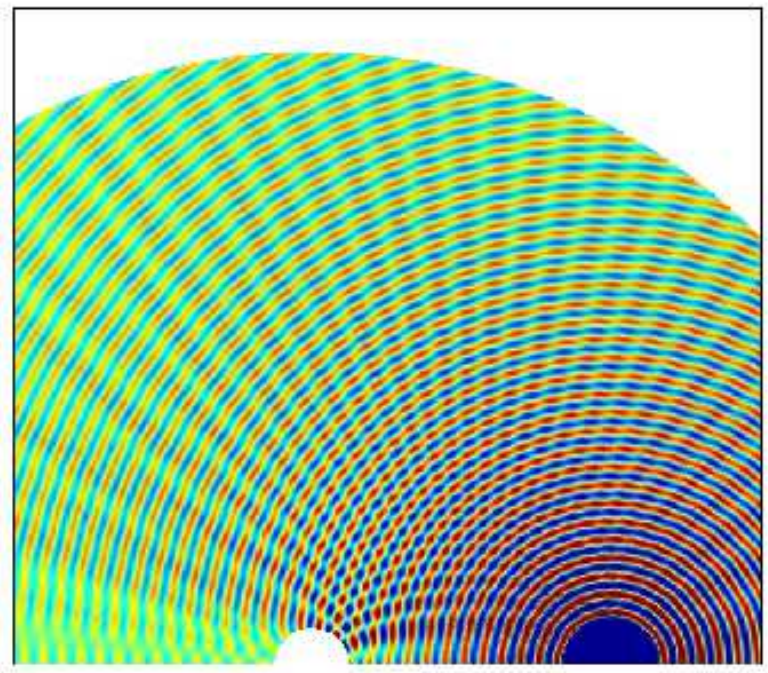

Cylinder, D=1, located at $(0, 0)$, periodic non-compact source located at $(4, 0)$, with $\omega = 8\pi$.

Comparison of computed and analytical directivity at $r = 7.5$.

Non-centred finite difference schemes

Example of importance of non-centred schemes.

2D scattering problem, from the Second Computational Aeroacoustics Workshop.

Centred, $\sigma_f = 0.2$

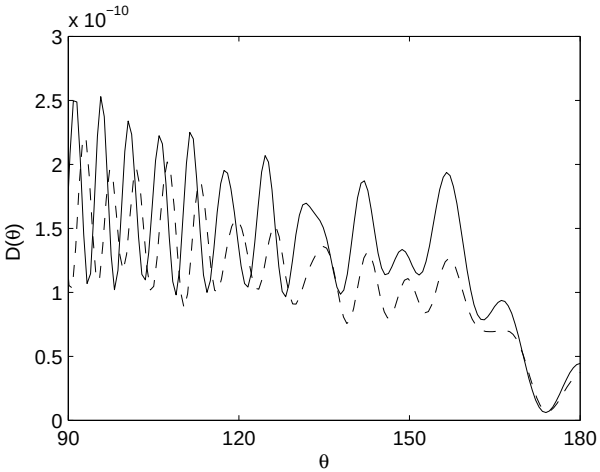

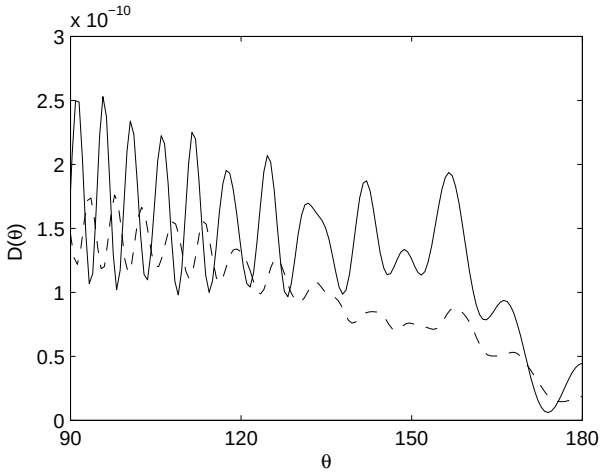

Centred, $\sigma_f = 0.8$

Optimised, $\sigma_f = 0.2$

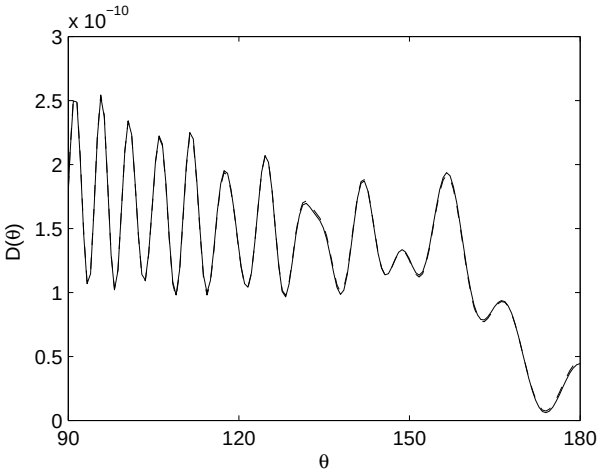

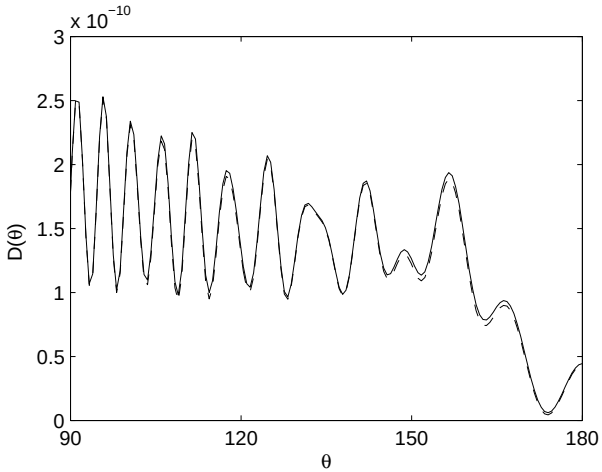

Optimised, $\sigma_f = 0.8$

Chimera grids and interpolation

A single curvilinear grid does not allow the description of complicated geometries. For complex geometries to be treated with finite difference techniques, two possibilities:

- immersed boundary approach
- multiple overlapping *chimera* grids and interpolation

Chimera grids and interpolation

A single curvilinear grid does not allow the description of complicated geometries. For complex geometries to be treated with finite difference techniques, two possibilities:

- immersed boundary approach
- multiple overlapping *chimera* grids and interpolation

Multi-body scattering example, from the 4^{th} CAA workshop, solved via **centred** Lagrange polynomial interpolation.

Chimera grids and interpolation

A single curvilinear grid does not allow the description of complicated geometries. For complex geometries to be treated with finite difference techniques, two possibilities:

- immersed boundary approach
- multiple overlapping *chimera* grids and interpolation

Multi-body scattering example, from the 4th CAA workshop, solved via **centred** Lagrange polynomial interpolation.

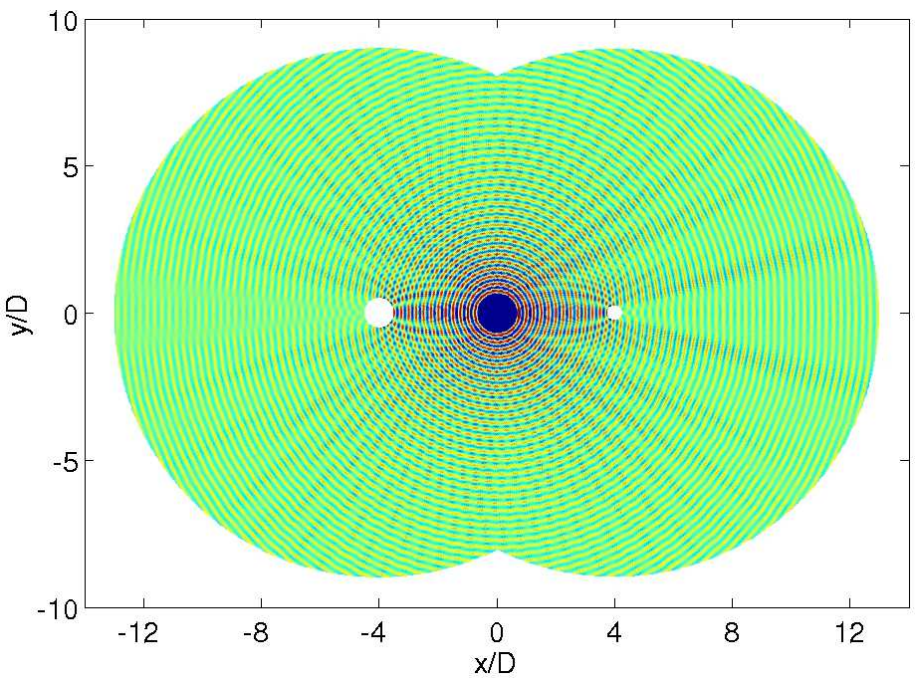

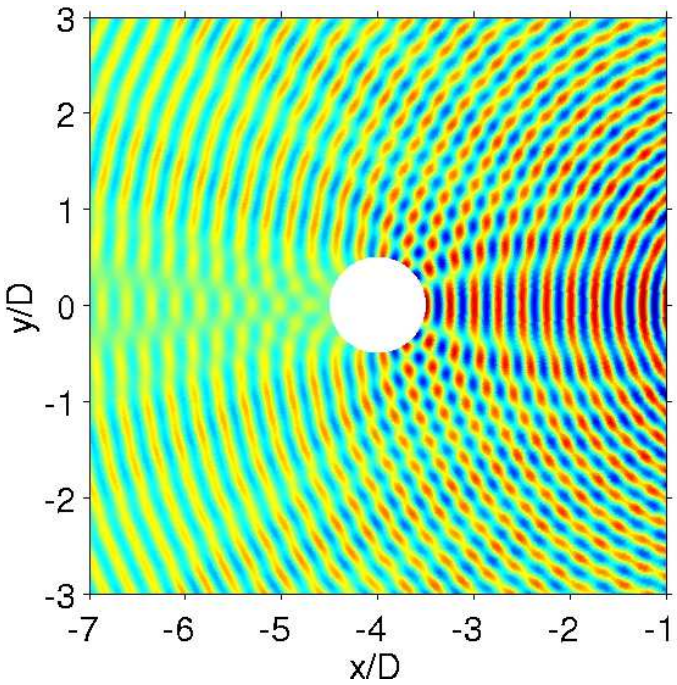

Chimera grids and interpolation

A single curvilinear grid does not allow the description of complicated geometries. For complex geometries to be treated with finite difference techniques, two possibilities:

- immersed boundary approach
- multiple overlapping *chimera* grids and interpolation

Multi-body scattering example, from the 4th CAA workshop, solved via **centred** Lagrange polynomial interpolation.

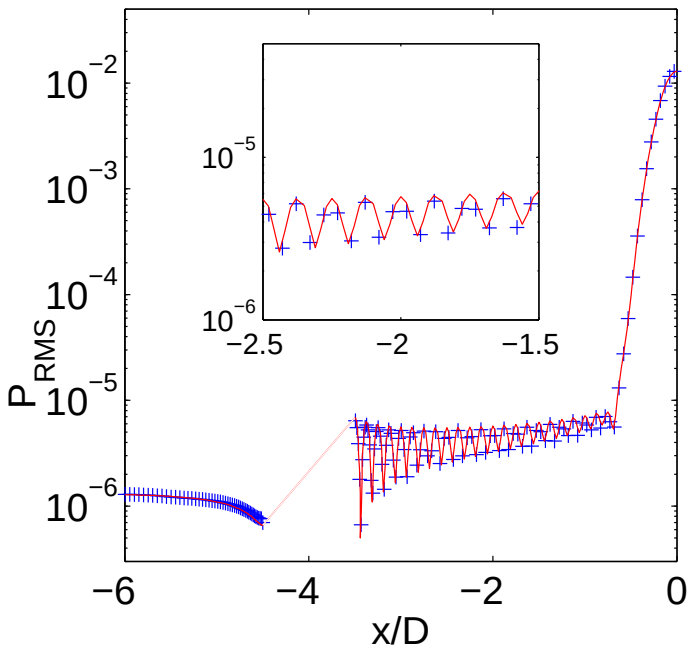

Non-centred interpolation

When interpolation needs to be carried out near a solid wall or boundary, large centred stencils cannot be used.

Non-centred interpolation

When interpolation needs to be carried out near a solid wall or boundary, large centred stencils cannot be used.

Non-centred Lagrange polynomial interpolation is unstable.

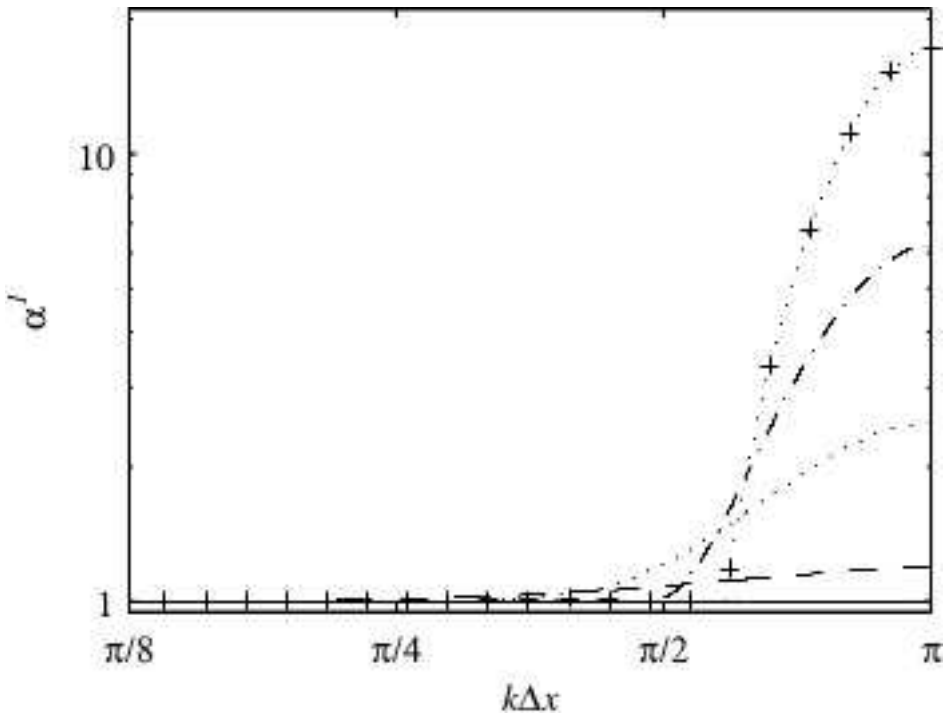

Amplification of Lagrange polynomial interpolation with 2-, 4-, 6-, 8- and 10-point stencils, donor point in first cell.

Non-centred interpolation

When interpolation needs to be carried out near a solid wall or boundary, large centred stencils cannot be used.

Optimised high-order non-centred interpolation is still unstable.

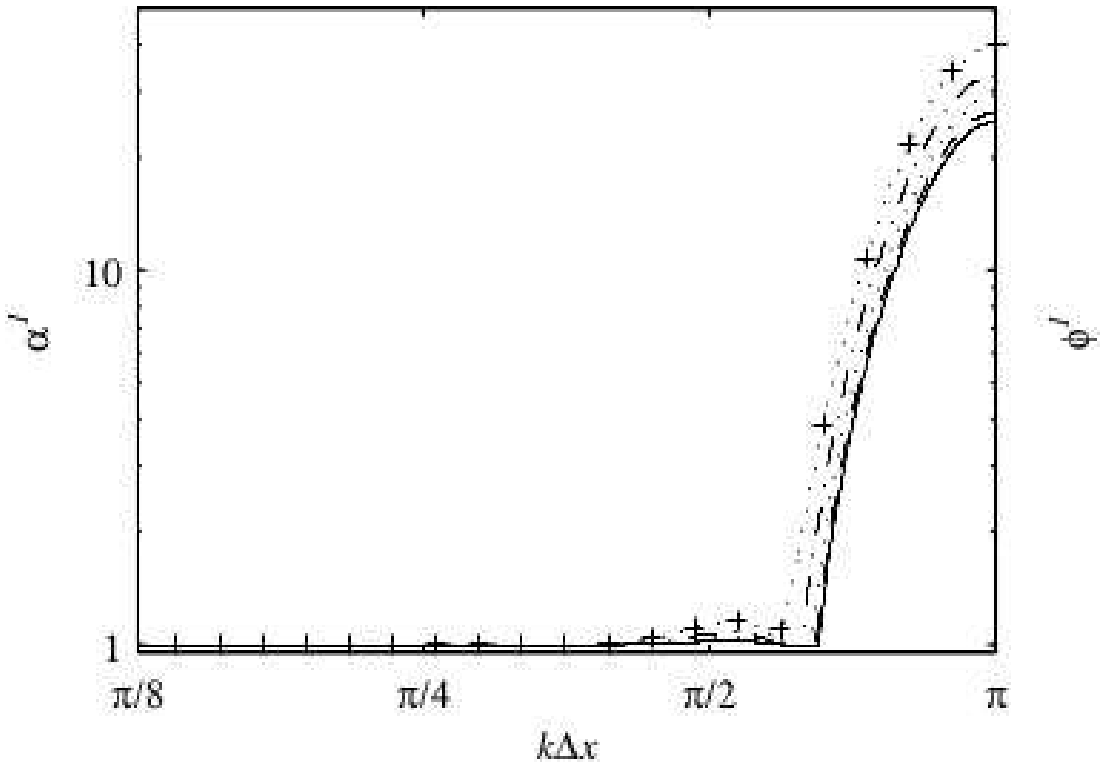

Amplification of optimised 12-point interpolation of orders 2, 4, 6, 8 and 10.

Non-centred interpolation

When interpolation needs to be carried out near a solid wall or boundary, large centred stencils cannot be used.

Constrained optimised high-order non-centred interpolation allows amplification to be controlled.

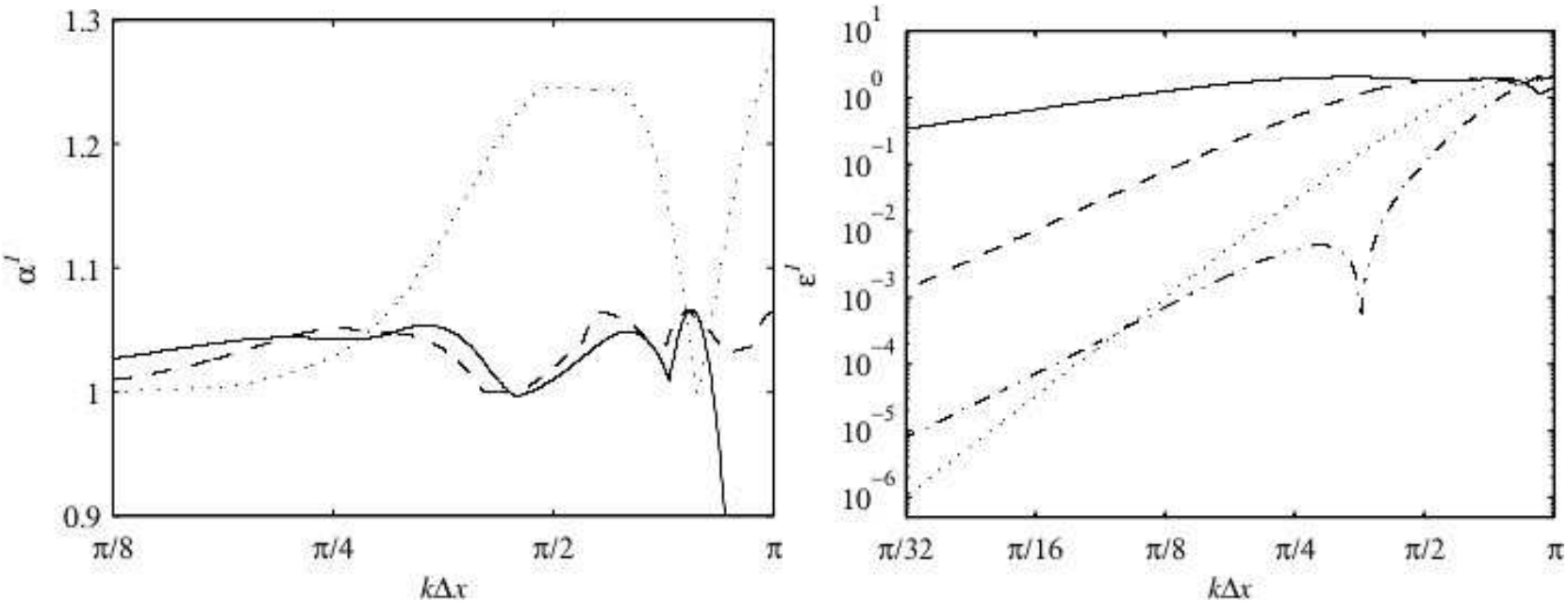

Amplification and error magnitude of constrained optimised 6-point interpolation stencils of orders 1, 3, 5, and error of non-constrained optimised 6-point 3rd order stencil.

Non-centred interpolation

Generation of constrained schemes.

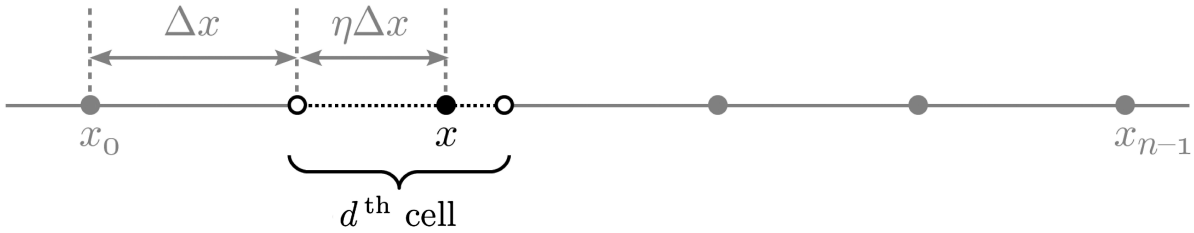

We choose to limit a scheme's amplification by imposing:

$$\forall k\Delta x, \alpha_{loc}(\eta, k\Delta x) \leq 1 + \alpha_{tol}$$

This inequality is hard to work with, and therefore transformed to an equality :

$$\|\alpha_{loc}(\eta, k\Delta x)\|_\infty = \max \alpha_{loc}(\eta, k\Delta x) = 1 + \alpha_{tol}$$

The infinite norm is then approximated by an L^{2q} norm, allowing the amplification constraint to be differentiated w.r.t. scheme coefficients and Lagrange multipliers:

$$\|\alpha_{loc}\|_{2q} = \left(\int_0^\pi (\alpha_{loc}(\eta, k\Delta x))^{2q} d(k\Delta x) \right)^{1/2q} = 1 + \alpha_{tol}$$

The value of α_{tol} is chosen as small as possible, and determined empirically.

Desvigne *et al*, SIAM J. Sci. Comput. 32(4), 2010

Non-centred interpolation

Finally the resulting (non-linear) Lagrangian multiplier problem is solved thanks to a Newton-Raphson approach for a discretized distribution of η.

Constrained optimisation

- allows stabilised accurate non-centred interpolation to be deployed in FD computations
- is cumbersome to develop, acceptable to use
  schemes are pre-calculated once and for all, and piecewise-polynomial regression is used in a calculation to determine values for a given donor position η
- could be used to generate improved boundary differencing schemes and filters (remains to be done!)

Cylindrical cavity flows

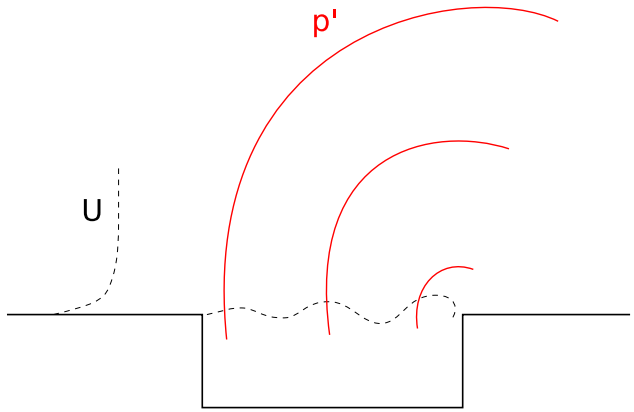

Fuel pressure vent on an A319

Cylindrical cavity flows

Geometry requires chimera approach for finite differences simulation.

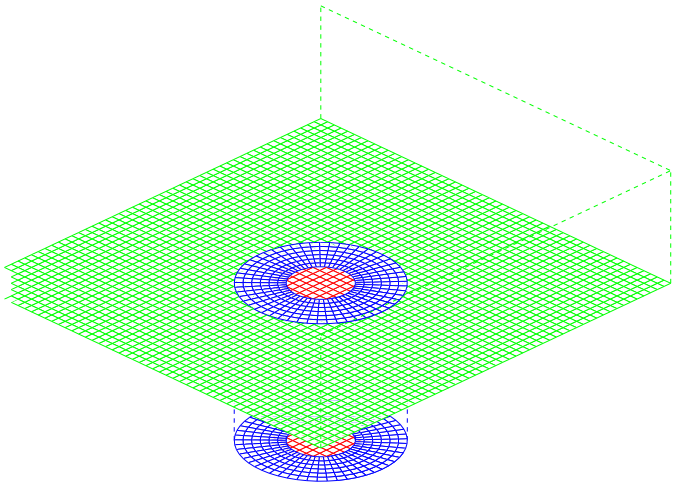

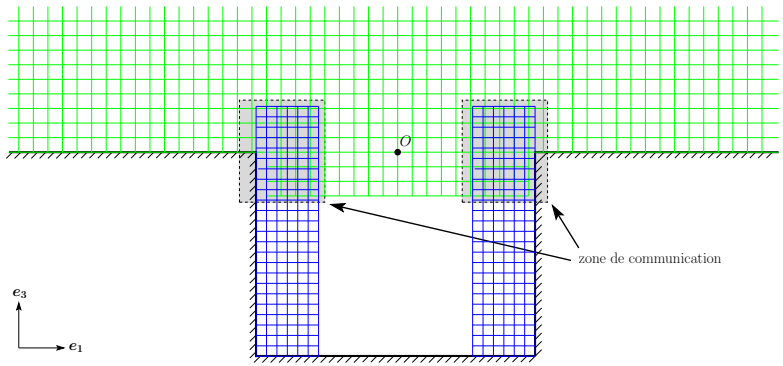

Grid structure used for computation of flow around cylindrical cavity.

Desvigne *et al*, SIAM J. Sci. Comput. 32(4), 2010

Cylindrical cavity flows

Experimental study characterised noise generation, a model coupling cavity depth resonance with shear layer dynamics was compared to successfully to data, and computations have since allowed previously untestable elements of the model to be checked.

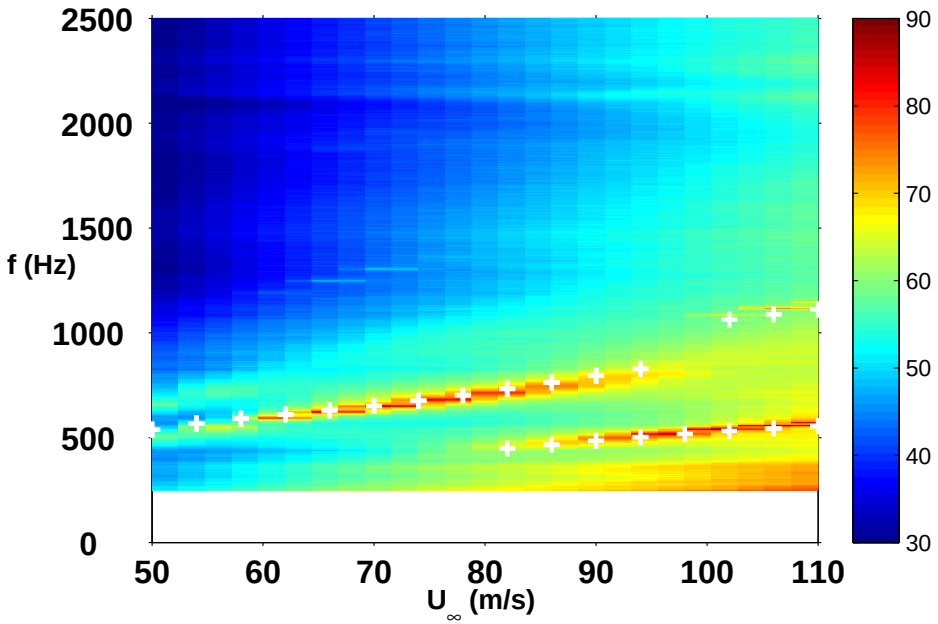

Predicted frequencies shown as white crosses

Far-field SPL for cavity of depth $h = 10$ cm.

Marsden *et al*, JSV 331 2012

Cylindrical cavity flows

Experimental study characterised noise generation, a model coupling cavity depth resonance with shear layer dynamics was compared to successfully to data, and computations have since allowed previously untestable elements of the model to be checked.

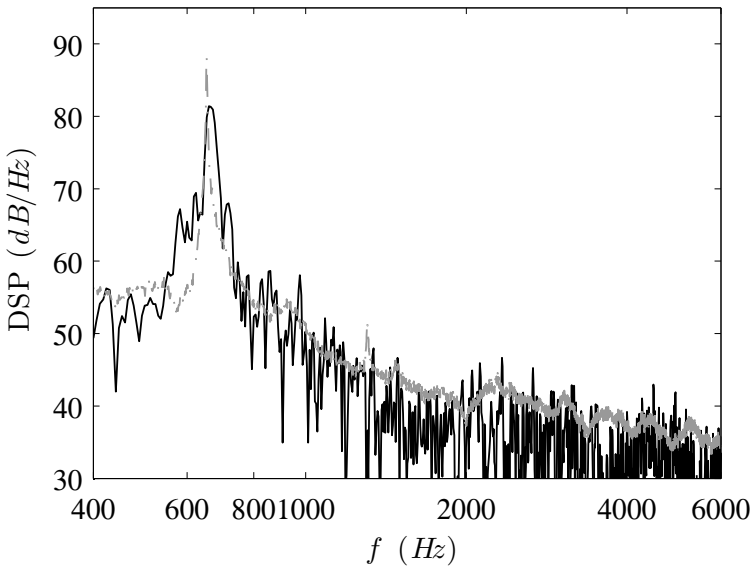

PSD (Pa^2/Hz) at 1 m above the cavity for $U_\infty = 70\,m/s$:

— experimental data

— computational data

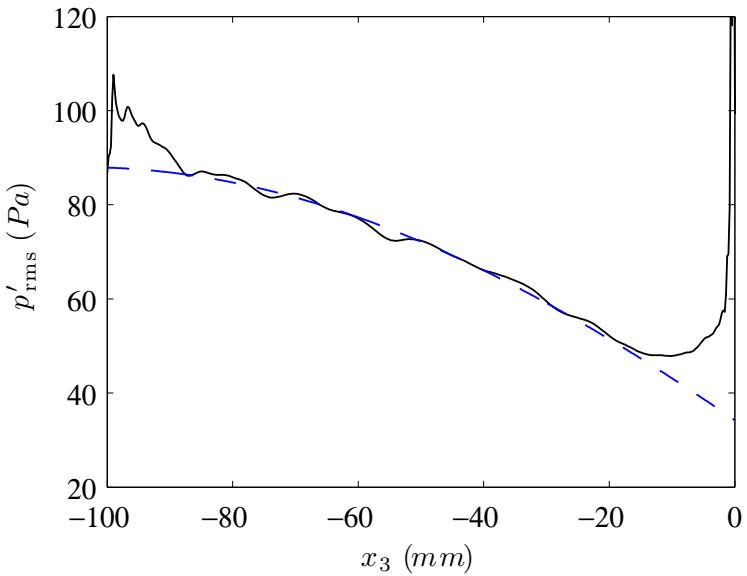

RMS pressure on upstream cavity wall as a function of depth.

Asymmetric mean flow in shallow cylindrical cavities

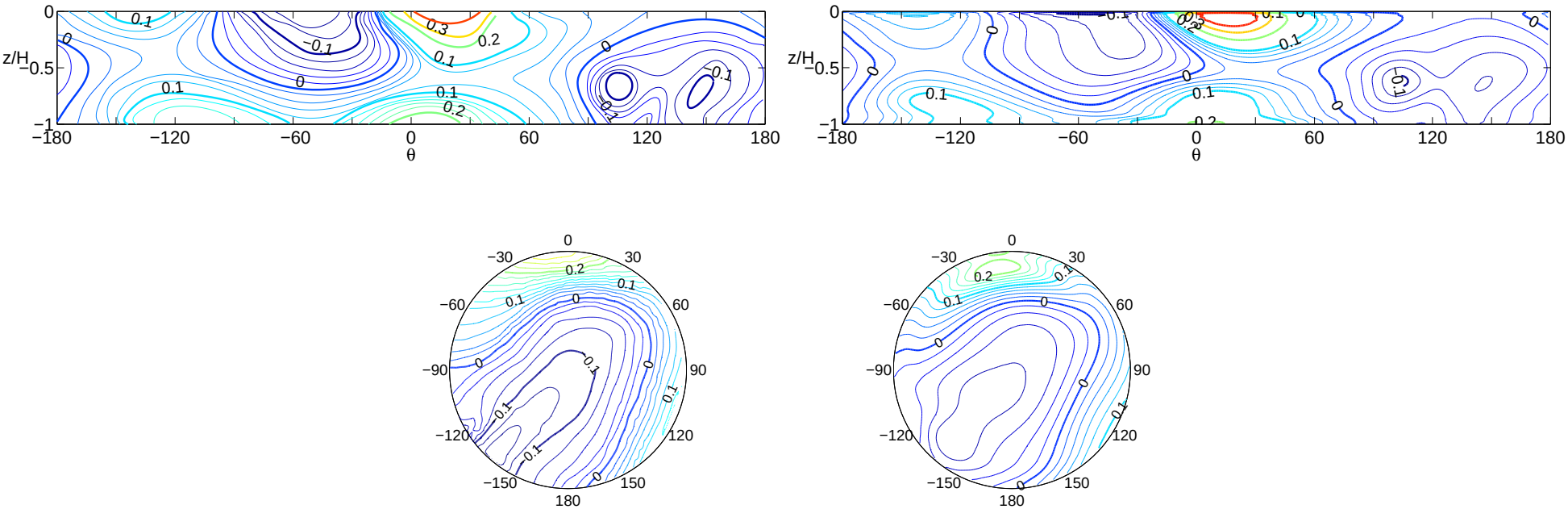

Static pressure coefficient on the cavity wall and floor for a cavity of depth $\kappa = H/D = 0.5$. Hiwada's data* at $M = 0.07$ (left), and computational data at $M = 0.25$ (right).

* Hiwada *et al*, JSME Bulletin 1983, vol 26(220) Marsden *et al*, Phys. Fluids 24, 2012

Asymmetric mean flow in shallow cylindrical cavities

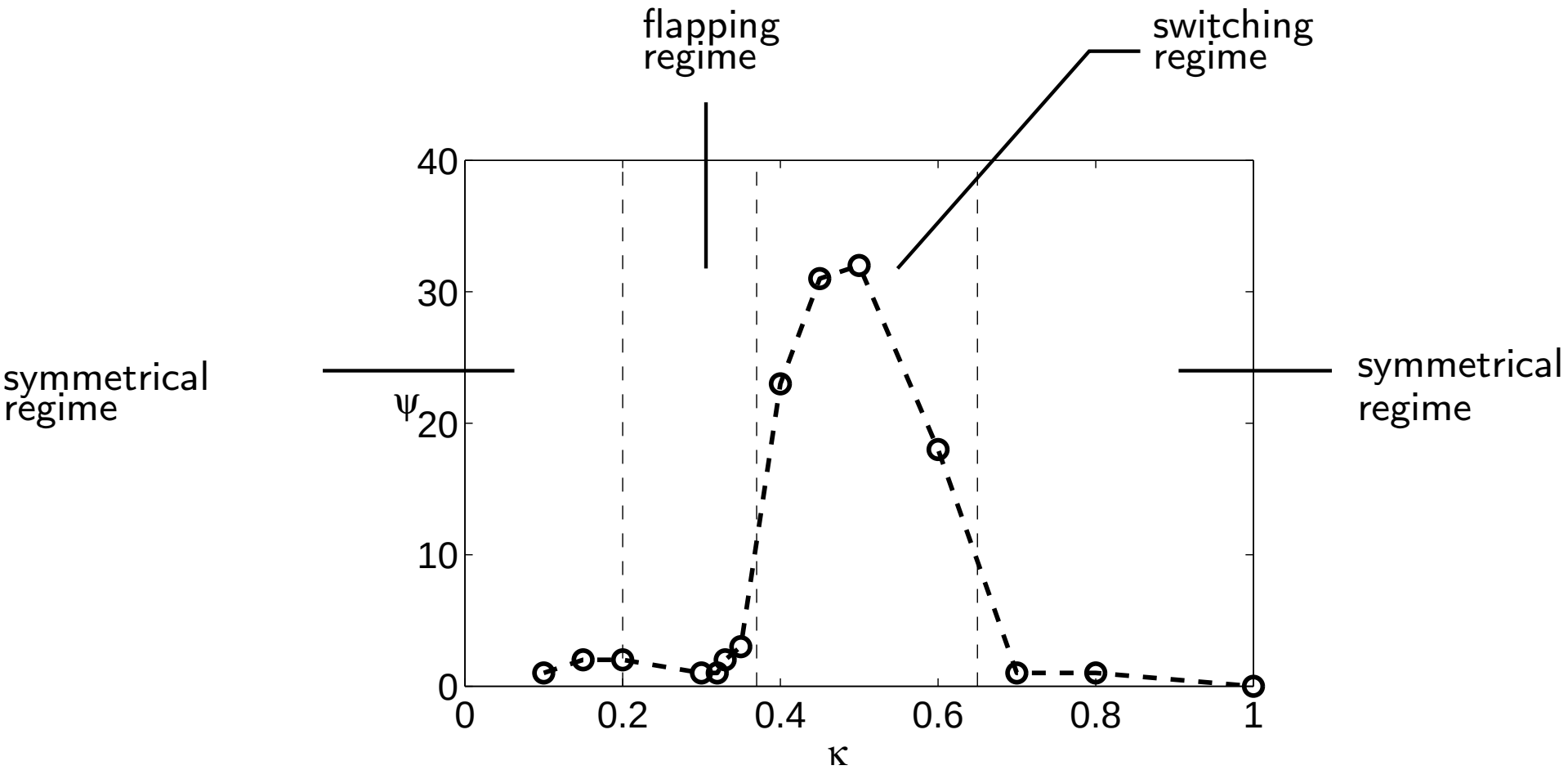

Mean flow rotation Ψ in degrees around the z axis as a function of cavity depth ratio $\kappa = H/D$, estimated from computations.

Flow flapping

For cavity depths between $\kappa \simeq 0.2$ and $\kappa \simeq 0.4$, *flow flapping* has been observed experimentally[*+], and is illustrated here with static pressure from the cavity wall:

[*] Hiwada *et al*, JSME Bulletin 1983, vol 26(220) [+] Dybenko & Savory, JAE 2008 vol 222(1)

Flow flapping

For cavity depths between $\kappa \simeq 0.2$ and $\kappa \simeq 0.4$, *flow flapping* has been observed experimentally*+, and is illustrated here with static pressure from the cavity wall:

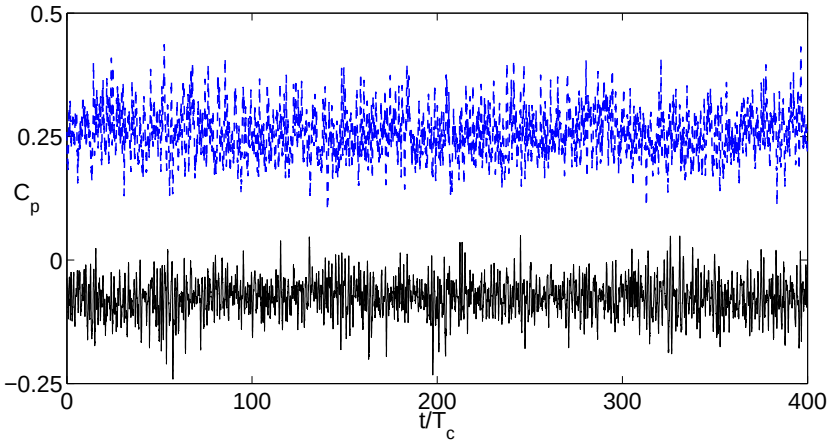

depth $\kappa = 0.5$

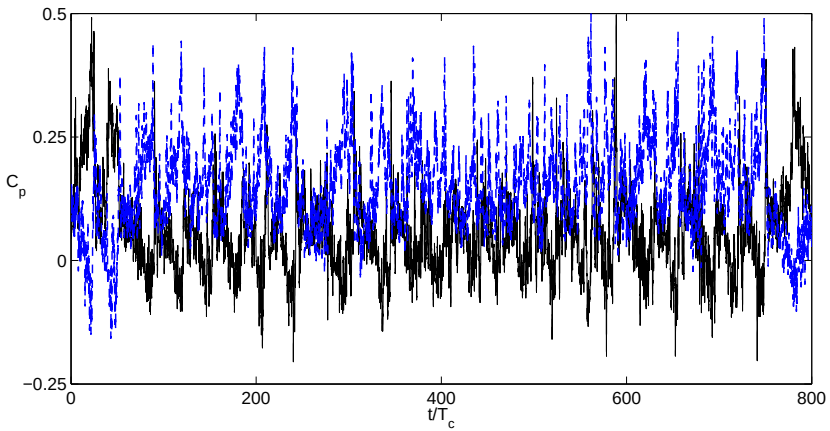

depth $\kappa = 0.32$

T_c: free stream convection time across the cavity $T_c = D/U_\infty$

* Hiwada *et al*, JSME Bulletin 1983, vol 26(220) + Dybenko & Savory, JAE 2008 vol 222(1)

Infrasound propagation

Context:
What infrasound signature does a large explosion generate?

A difficult problem

- very large propagation distances (100s to 1000s of wavelengths, 100s of km) frequencies of interest : 0.01 - 0.5 Hz
- over these distances, the atmosphere is highly inhomogeneous and stratified
- vertical temperature gradient induces strong downwards refraction and wave-guiding
- gravity stratification leads to highly non linear propagation in the high atmosphere, irrespective of source amplitude

Infrasound propagation

Atmospheric profiles

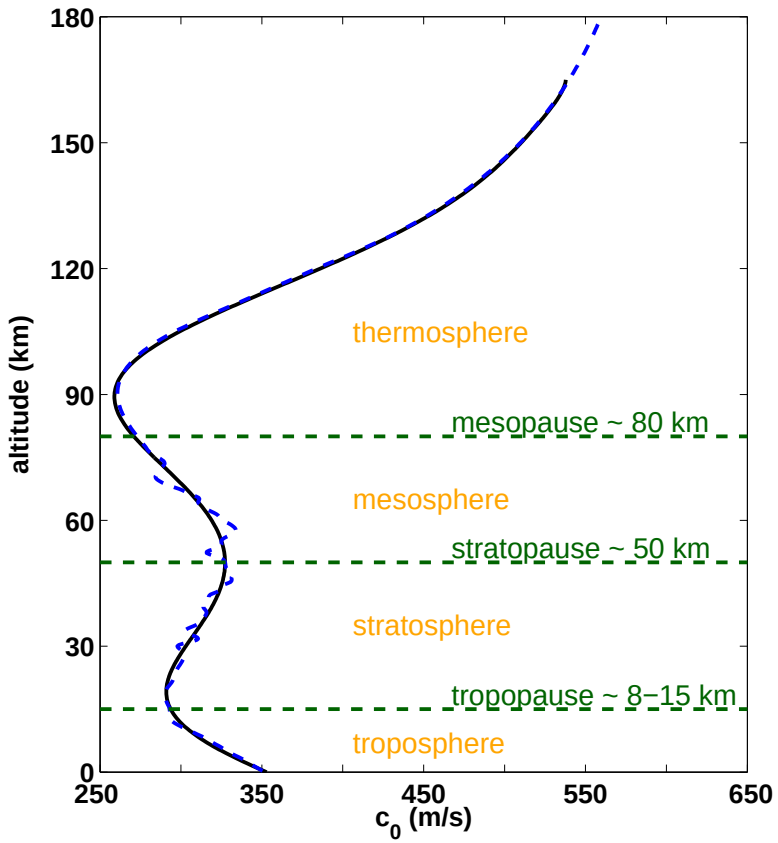

pressure profile is obtained by integrating the hydrostatic equation

$$\ln(\overline{p}/p_0) = -\frac{gM}{R}\int_0^z \frac{1}{\overline{T}}dz$$

Integration of this equation must be performed with care:

we must respect $\widetilde{\frac{d\overline{p}}{dz}} = -\rho g$ where $\widetilde{\frac{d}{dz}}$ is numerically approximated derivative.

Misty Picture computation

Example sound field

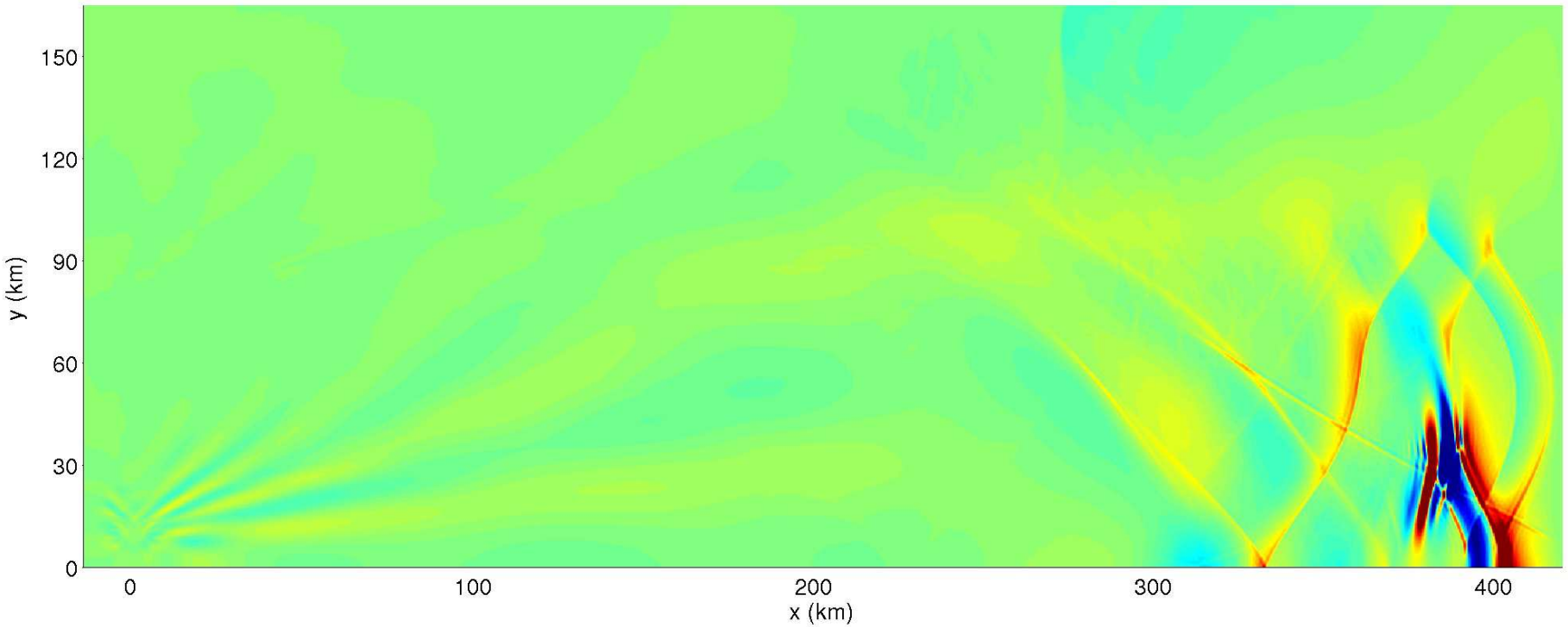

Scaled pressure field $p/\sqrt{\rho}$ 1320 s after detonation.

Misty Picture computation

Example sound field

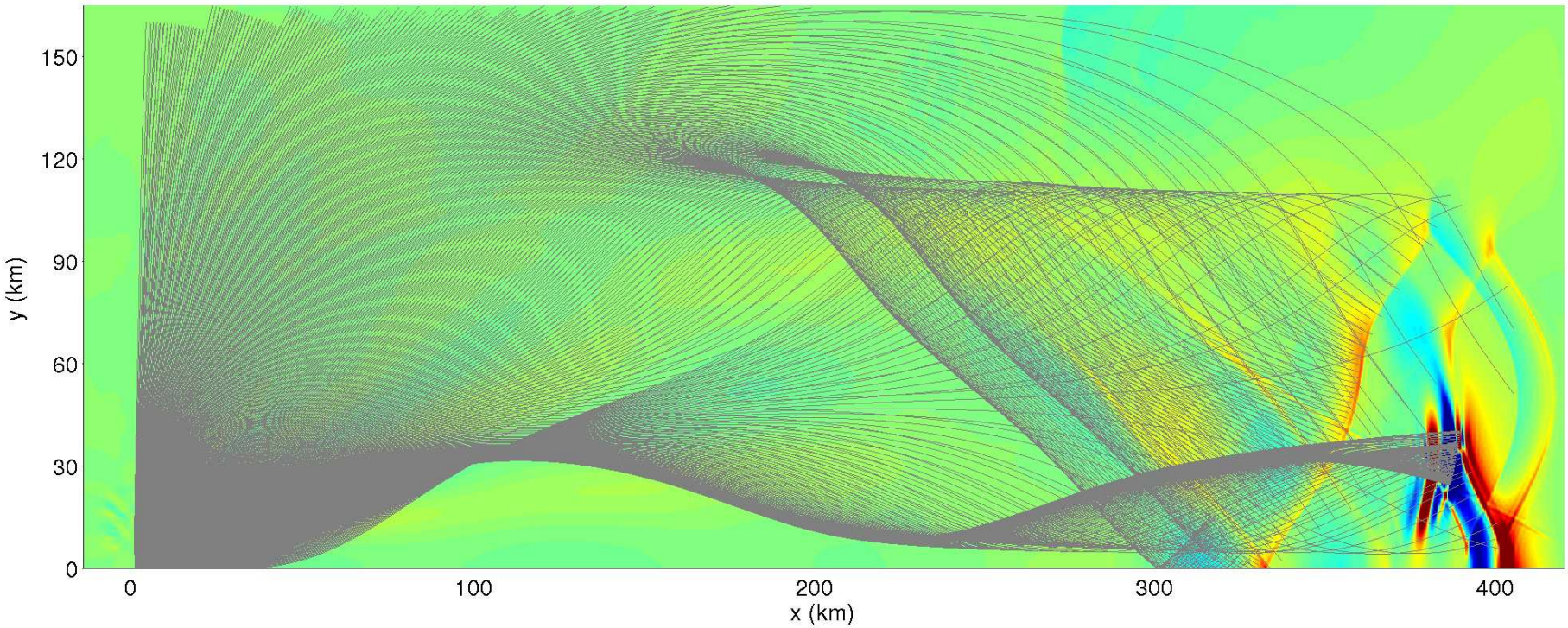

Scaled pressure field $p/\sqrt{\rho}$ 1320 s after detonation.

Misty Picture computation

Quantitative results

Signals are compared at ground level 400km away from the source:

Misty Picture computation

Quantitative results

Signals are compared at ground level 400km away from the source:

- weakest signal remains linear throughout the propagation
- strongest signal exhibits strong non-linear effects

Misty Picture computation

Quantitative results

Signals are compared at ground level 400km away from the source:

- weakest signal remains linear throughout the propagation
- strongest signal exhibits strong non-linear effects

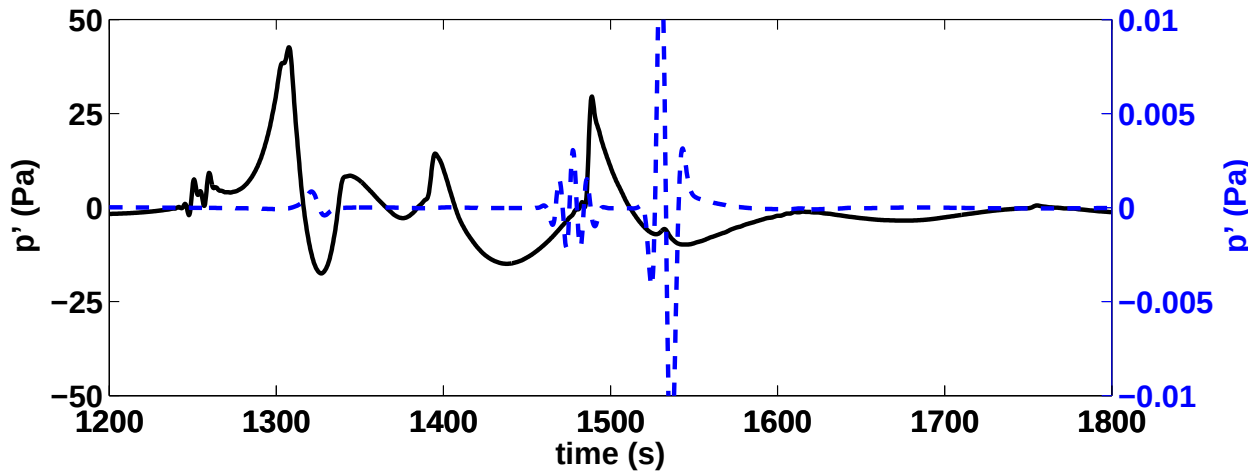

Pressure fluctuations for source amplitudes $\mathcal{A} = 5000$ Pa (left axis) and $\mathcal{A} = 0.005$ Pa (right axis).

Misty Picture computation

Source amplitude effects - I

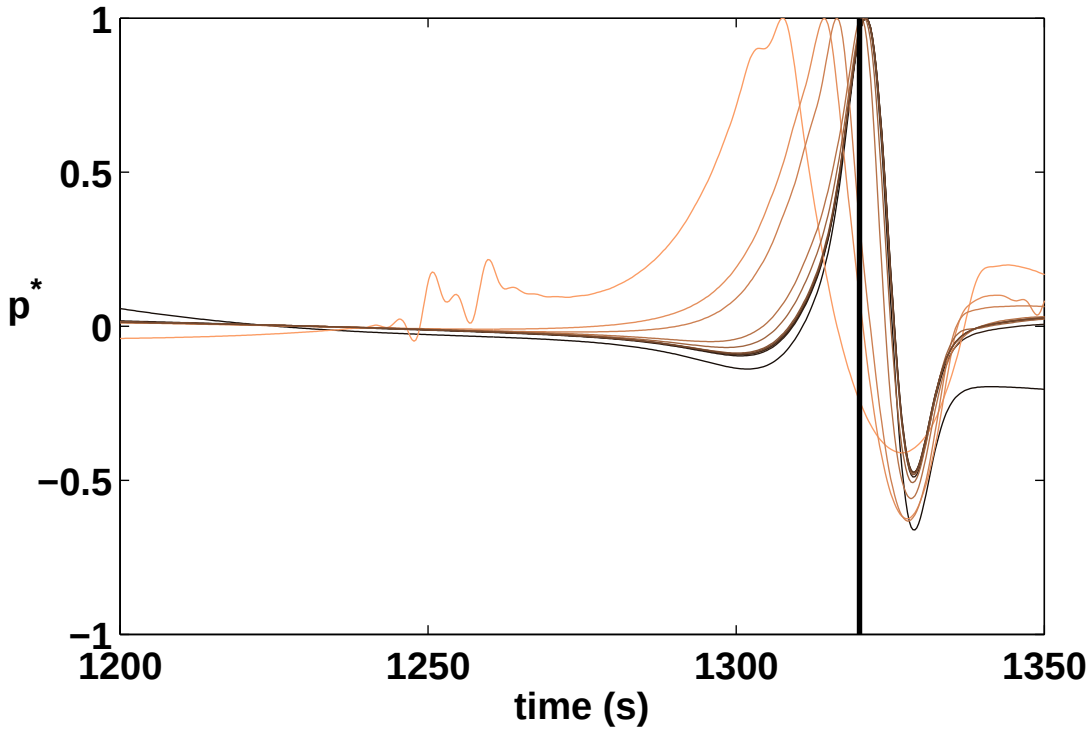

p^*: pressure normalized by amplitude of first eigenray arrival

Misty Picture computation

Source amplitude effects - II

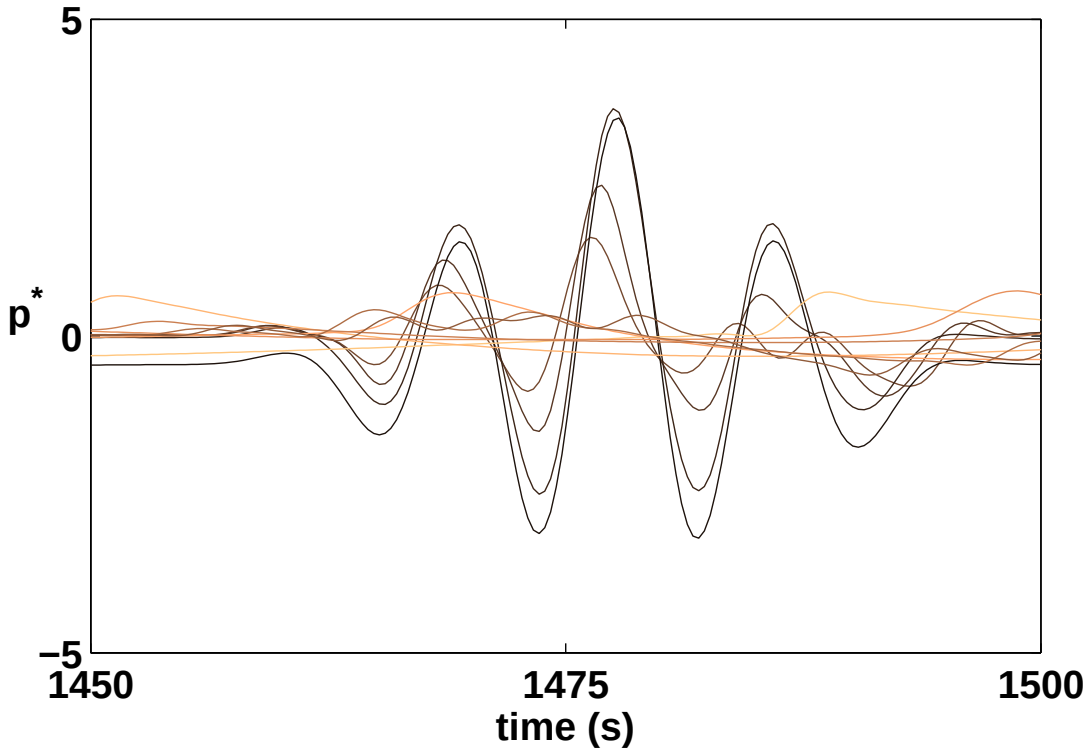

p^*: pressure normalized by amplitude of first eigenray arrival

Misty Picture computation

Source amplitude effects - III

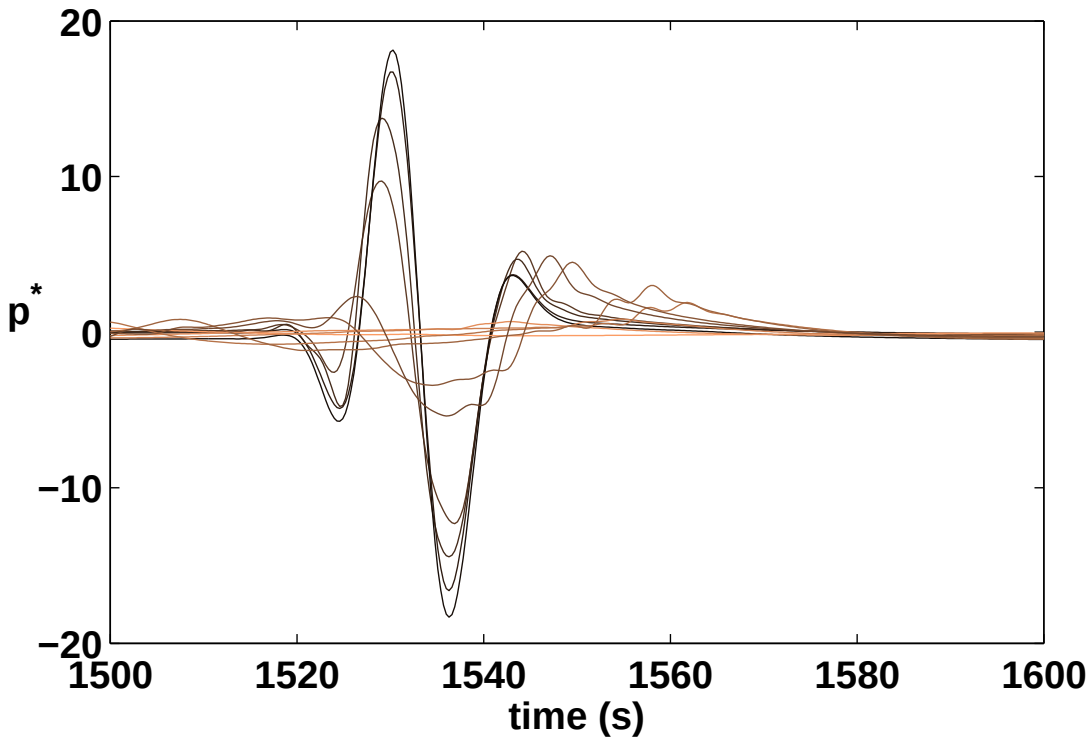

p^*: pressure normalized by amplitude of first eigenray arrival

Misty Picture computation

Source amplitude effects - III

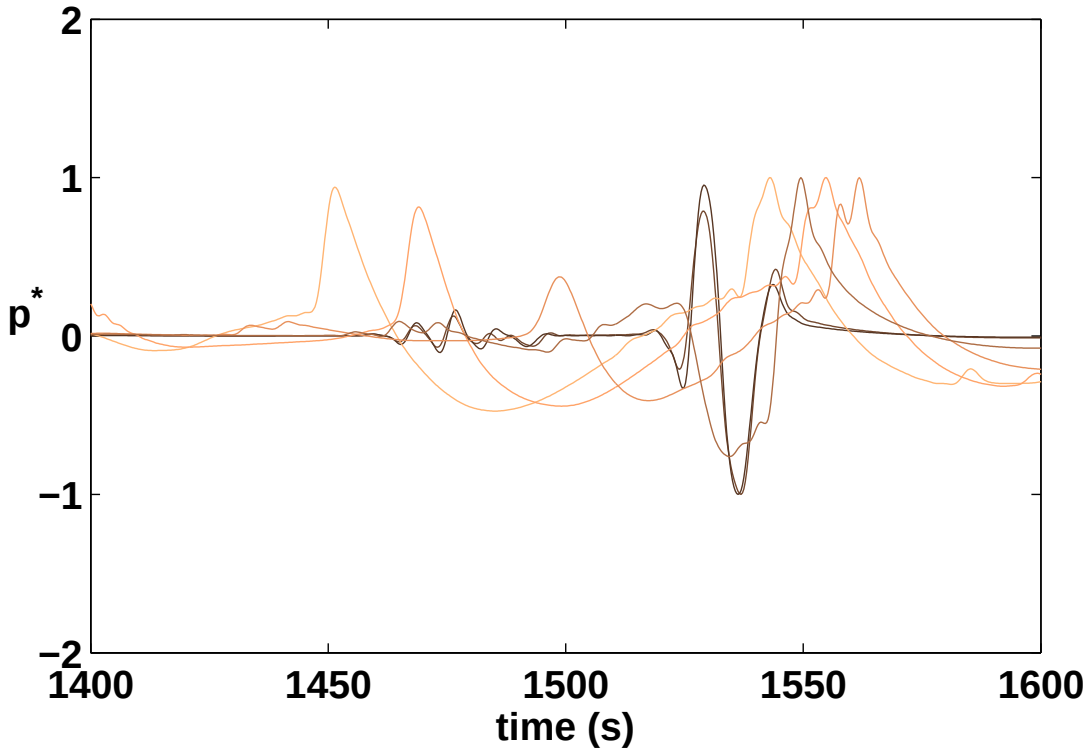

p^*: pressure normalized by amplitude of thermospheric eigenray arrival

Misty Picture computation

Visco-thermal effects

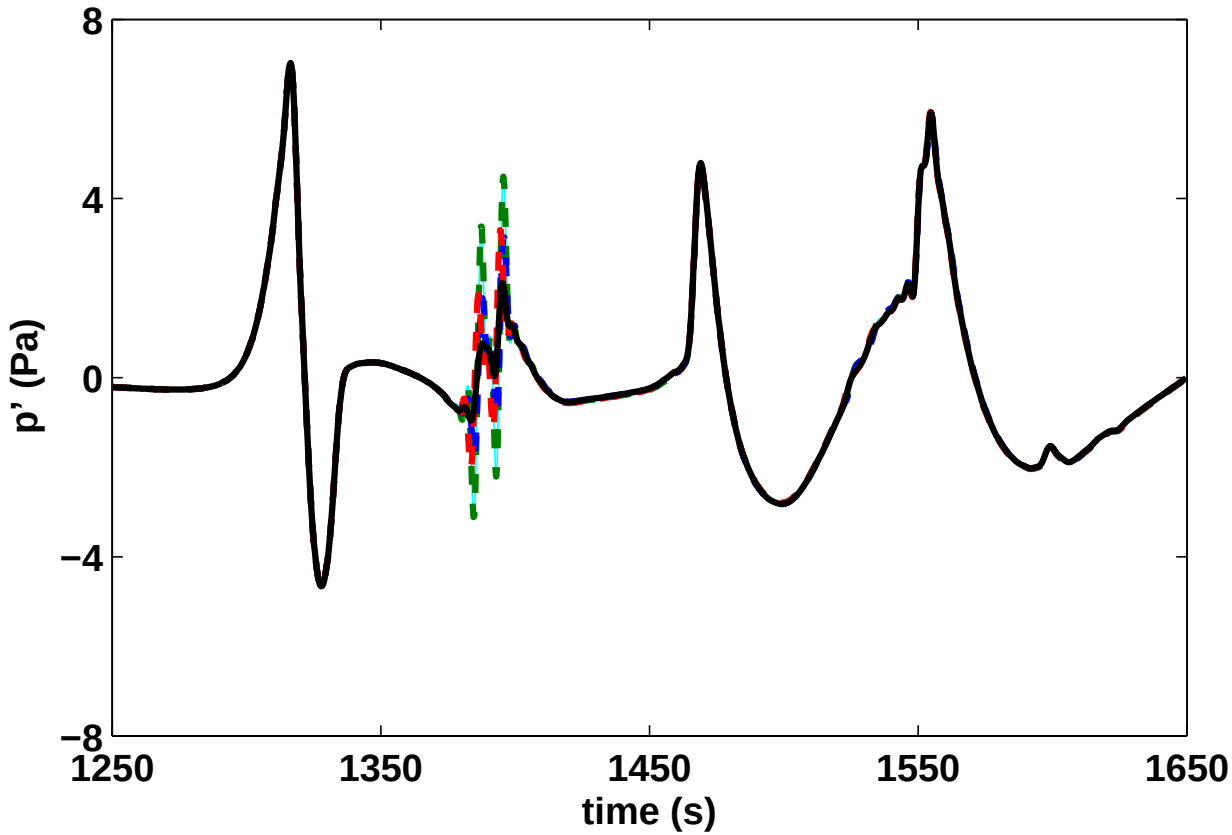

– total computation, - - computation without heat conduction,
- - computation without viscous damping, - - non-linear Euler computation

Misty Picture computation

Visco-thermal effects

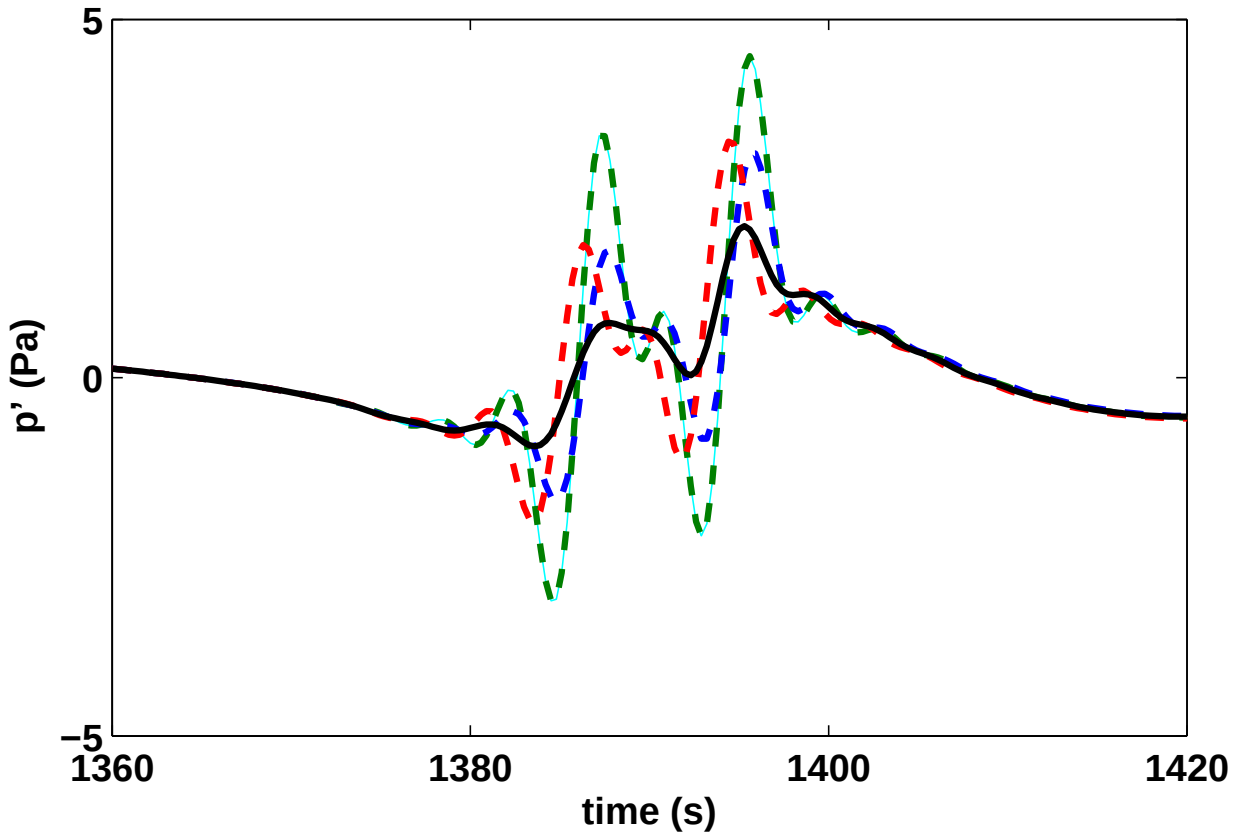

– total computation, - - computation without heat conduction,
- - computation without viscous damping, - - non-linear Euler computation

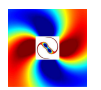

Airfoil noise

- Unsteady flow crossing a trailing edge is a common source of noise. There are numerous published experimental studies for NACA airfoils, and LES techniques & computing resources are getting to the point where noise generation can be accurately predicted.

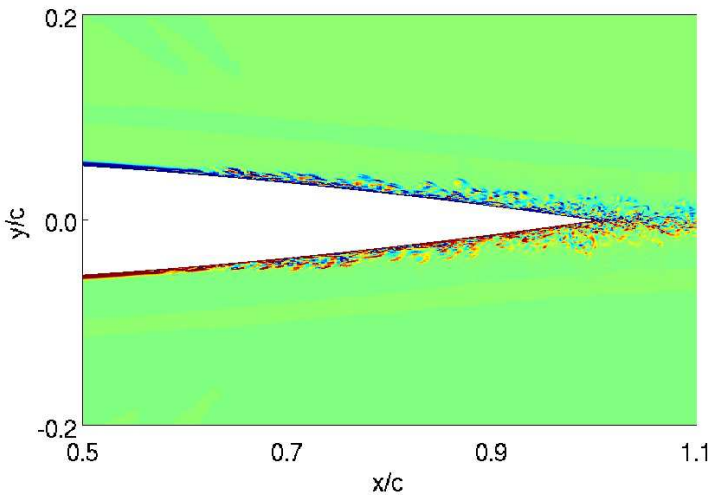

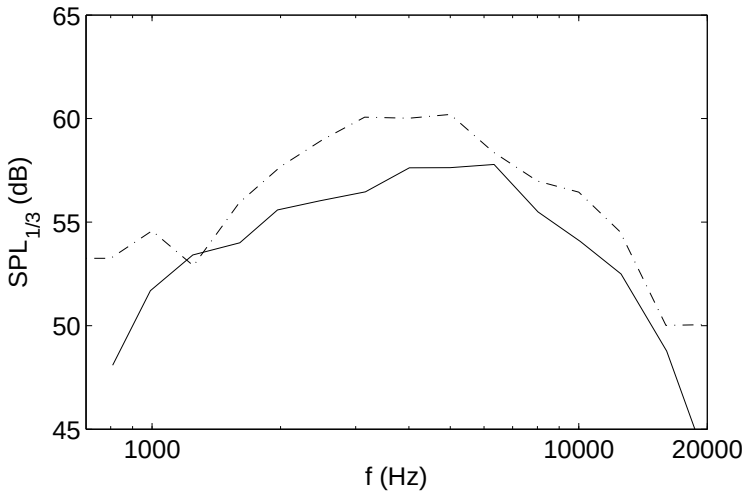

Vorticity around the trailing edge of a NACA 0012 airfoil at Re=500,000, and comparison of resulting acoustic far field with experimental data.

Marsden *et al*, AIAA J. 46(4), 2008

Airfoil noise

- Unsteady flow crossing a trailing edge is a common source of noise. There are numerous published experimental studies for NACA airfoils, and LES techniques & computing resources are getting to the point where noise generation can be accurately predicted.
- NACA airfoils are known to generate acoustic tones for a range of low chord based Reynolds numbers.

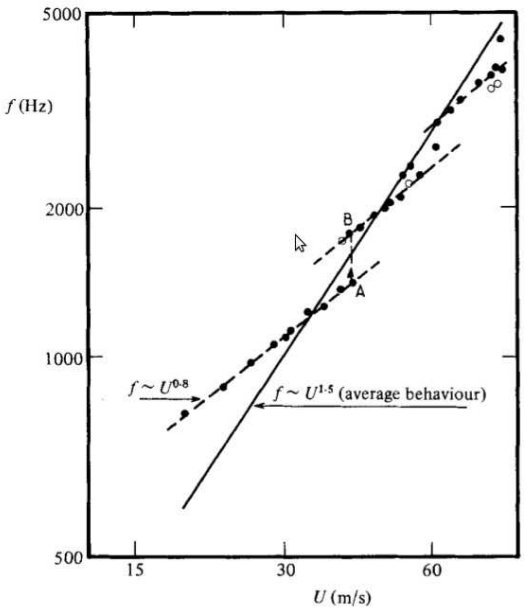

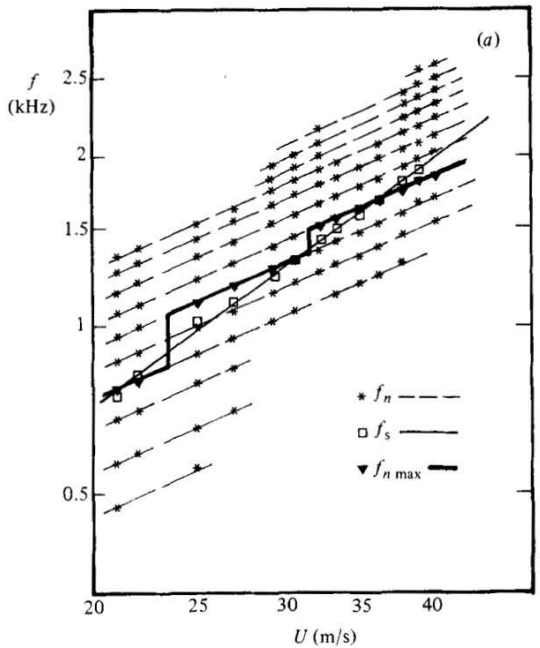

Airfoil noise - recent work

Parametric study on Reynolds number and Mach number influence.

- Reynolds numbers range from 10,000 to 100,000,
- Mach numbers from M=0.15 to M=0.5,
- the airfoil chord c from 2×10^{-3} to 6×10^{-3} mm,
- and the angle of attack from 0 to 4 degrees.

Current question : what are the tonal characteristics for these Reynolds numbers?

Airfoil noise - ongoing work

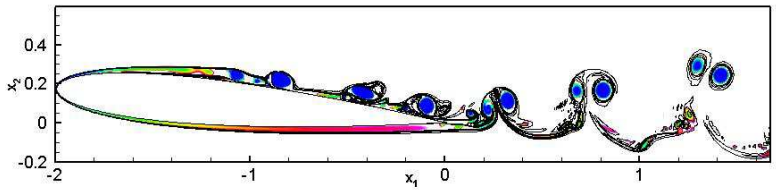

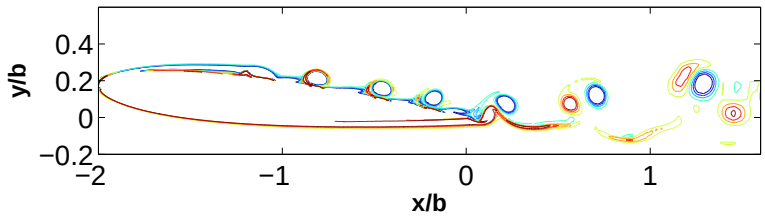

Contour lines of instantaneous vorticity field for a NACA 0012 airfoil at Re=50×10^3 and M=0.4. Left: figure from Sandberg *et al.*, right: present work.

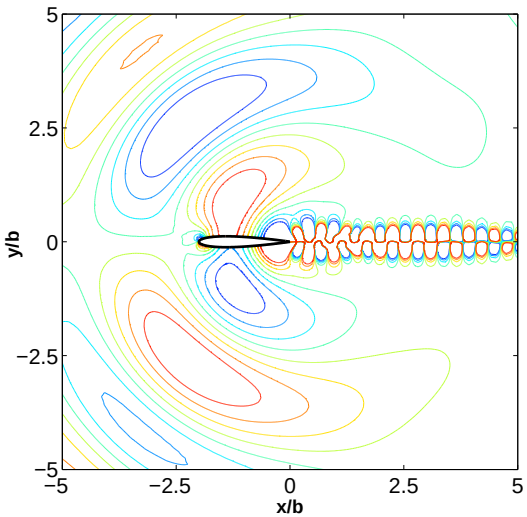

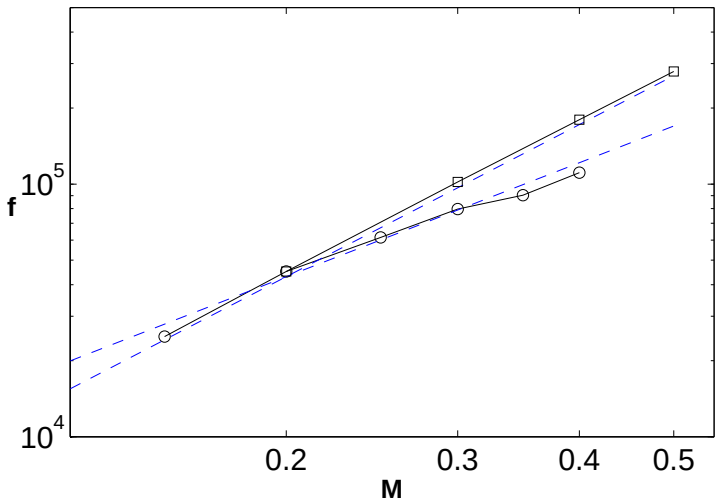

Left: instantaneous vorticity and pressure fields at M=0.15 and Re=17.4×10^3. Colour scales between $\pm 20 U_\infty / c$ s^{-1} for vorticity and ± 3 Pa for pressure

Right: frequencies as a function of Mach number at zero angle of attack, $\circ$ for an airfoil of chord $c = 5\times10^{-3}$ m and $\square$ for an airfoil at a constant Reynolds number of

High-order Finite Differences : progress in their usability

Alleviating the negative points

- wall schemes
  simple high-order (Taylor series) non centred FD schemes are highly unstable :
  $Im(k - k^*) \neq 0$
  alot of progress on generating stable high-order FD schemes has been achieved

High-order Finite Differences : progress in their usability

Alleviating the negative points

- wall schemes
- curvilinear grids

  on curvilinear grids, high order and high accuracy can be maintained everywhere, including at solid boundaries

High-order Finite Differences : progress in their usability

Alleviating the negative points

- wall schemes
- curvilinear grids
- interpolation techniques

  high accuracy straightforward to obtain for centred interpolation, non-centred needs special care to be stable

High-order Finite Differences : progress in their usability

Alleviating the negative points

- wall schemes
- curvilinear grids
- interpolation techniques
- regarding computational cost and modern hardware

High-order Finite Differences : progress in their usability

Alleviating the negative points

- wall schemes
- curvilinear grids
- interpolation techniques
- regarding computational cost and modern hardware
  - local spatial stencil reduces need for communication: only border points need synchronising

High-order Finite Differences : progress in their usability

Alleviating the negative points

- wall schemes
- curvilinear grids
- interpolation techniques
- regarding computational cost and modern hardware
  - local spatial stencil reduces need for communication: only border points need synchronising
  - allows for excellent scaling on large problems
    strong scaling estimated around 90% for latest jet computations running on 4,000 cores, 2 billion grid points; $\approx$ 2E-6 s / it / pt

High-order Finite Differences : progress in their usability

Alleviating the negative points

- wall schemes
- curvilinear grids
- interpolation techniques
- regarding computational cost and modern hardware
  - local spatial stencil reduces need for communication: only border points need synchronising
  - allows for excellent scaling on large problems
    strong scaling estimated around 90% for latest jet computations running on 4,000 cores, 2 billion grid points; $\approx$ 2E-6 s / it / pt
  - very well matched to recent graphics hardware
    - 512x128x64 domain shear layer runs at around 20 time steps / second on single GPU, used since september 2012 in teaching!

Conclusions

- Despite their reputation of being impractical, improvements in differencing, filtering and interpolation techniques in particular for non-centred use cases mean that they are now useable around (simple) real geometries.
- Three examples of problems where high-order finite differences have shown excellent results:
  - resonant cavity flow
  - long-distance infrasound propagation
  - low Reynolds number airfoil noise
- A lot can still be improved!